Distribution Agreement

In presenting this thesis as a partial fulfillment of the requirements for a degree from Emory University, I hereby grant to Emory University and its agents the non-exclusive license to archive, make accessible, and display my thesis in whole or in part in all forms of media, now or hereafter now, including display on the World Wide Web. I understand that I may select some access restrictions as part of the online submission of this thesis. I retain all ownership rights to the copyright of the thesis. I also retain the right to use in future works (such as articles or books) all or part of this thesis.

Nima Shariatzadeh April 7, 2021

Baseline Levels of Neuroinflammation in the Grin2a Knockout Mouse

by

Nima Shariatzadeh

Dr. Nicholas H. Varvel, PhD.
Adviser

Chemistry Department

Dr. Nicholas H. Varvel, PhD.
Adviser

Dr. Dennis C. Liotta, PhD.
Committee Member

Dr. Stephen F. Traynelis, PhD.
Committee Member

Dr. Asheebo Rojas, PhD.
Committee Member

Dr. Steven A. Sloan, MD., PhD.
Committee Member

2021

Baseline Levels of Neuroinflammation in the Grin2a Knockout Mouse

By

Nima Shariatzadeh

Dr. Nicholas H. Varvel, PhD.
Adviser

An abstract of
a thesis submitted to the Faculty of Emory College of Arts and Sciences
of Emory University in partial fulfillment
of the requirements of the degree of
Bachelor of Science with Honors

Department of Chemistry

2021

Abstract
Baseline Levels of Neuroinflammation in the Grin2a Knockout Mouse
By Nima Shariatzadeh

Epilepsy is a common neurological disease characterized by recurrent seizures. Genetic loss-of-function variants of *GRIN2A* are causative for epilepsy. *GRIN2A* encodes the GluN2A subunit of the NMDA receptor, a major glutamatergic excitatory receptor in the brain. A growing body of work has implicated neuroinflammation in the disease course of epilepsy, and deletion of the GluN2A subunit has been associated with neuroinflammation. In humans, anti-inflammatory agents are beneficial in *GRIN2A*-associated epilepsy; these patients experience normalized EEGs, improved language, and improved sleep architecture when administered anti-inflammatory therapies. However, no work to date has measured the effect of this receptor on baseline, non-epileptic neuroinflammation levels. Microglia and astrocytes are brain-derived glial cells that undergo morphological transformation during neuroinflammation. Using *Grin2a* knockout (KO) mice lacking the GluN2A subunit, neuroinflammation was measured via immunohistochemical staining of microglia and astrocytes using anti- IBA1 and GFAP antibodies, respectively, in both adolescent and adult mice. A slight, 1.36-fold increase in fluorescent area covered by GFAP staining was found in the CA1 radiatum of adolescent mice lacking the GluN2A subunit. No difference between genotypes was observed in GFAP staining in adults, nor was a difference found between genotypes for adolescent and adult IBA1 staining. These findings indicate that during development, there is a transient increase in astrocyte reactivity in Grin2a KO mice that resolves by adulthood.

Baseline Levels of Neuroinflammation in the Grin2a Knockout Mouse

By

Nima Shariatzadeh

Dr. Nicholas H. Varvel, PhD.
Adviser

A thesis submitted to the Faculty of Emory College of Arts and Sciences
of Emory University in partial fulfillment
of the requirements of the degree of
Bachelor of Science with Honors

Department of Chemistry

2021

Table of Contents

Figures

Tables

Introduction

Epilepsy

Epilepsy is one of the most common neurological disorders, and it is estimated that 30% of patients are refractory to current treatments (Duncan JS et al., 2006). Clinically, epilepsy is defined as a neurological disorder whereby a patient experiences two or more unprovoked seizures, more than 24 hours apart (Fisher RS et al., 2014). During a seizure, patients may experience changes in motor function, feelings, behavior, or consciousness (Blumenfeld H, 2012; Li Z et al., 2002; Masia SL and Devinsky O, 2000). The seizures are initiated by unregulated, highly synchronous hyperexcitability that begins in one region of the brain and can then spread to other regions (Babb TL et al., 1987). Many anti-glutamatergic agents are used in the treatment of certain seizures, and glutamate receptors such as NMDA receptors play a role in the changes in plasticity and neuronal cell loss that follow these seizures (Kapur, 2018).

Glutamate and Glutamate Receptors

Glutamate is the primary excitatory neurotransmitter in the adult mammalian central nervous system (CNS). This amino acid neurotransmitter binds to two different types of receptors: metabotropic and ionotropic receptors (Platt SR, 2007). All eight subtypes of metabotropic glutamate receptors are G-protein-coupled receptors (GPCRs) that participate in intracellular signaling. There are three known sub-families of ionotropic receptors that bind glutamate; kainate, AMPA, and NMDA receptors (Kew JN and Kemp JA, 2005). Kainate receptors can be both pre and post-synaptic and modulate both excitatory and inhibitory firing (Lerma J, 2003). The α-amino-3-hydroxy-

5-methyl-4-isoxazolepropionic acid receptor (AMPAR) is a heterogenous post-synaptic excitatory receptor that mediates nearly all fast excitatory neurotransmission in the CNS. The receptors play a role in synapse formation, stabilization, and plasticity. These receptors colocalize to NMDA in the post-synaptic density. (Henley JM and Wilkinson KA, 2016). Finally, the N-methyl-D-Aspartate receptor (NMDAR) is the third kind of ionotropic glutamate receptor. It is a tetrameric (GluN) receptor, consisting of two obligate N1 subunits and some combination of N2 (A-D) or N3 (A-B) subunits., The presence of different subunits confers different properties to the NMDA receptor (Paoletti P et al., 2013). These receptors are blocked by magnesium and when this occurs only a sufficiently strong decrease in the polarization of the neuron can remove the magnesium block of the receptor and allow calcium or sodium ions to flow through it. The NMDA receptor binds 2 ligands (glutamate and glycine) that act as co-agonists (Xin WK et al., 2005; Zhu S et al., 2016).

NMDA Receptor Subunit Expression in the Brain

The NMDA receptor is primarily known for its function in learning and memory via its role in synaptic plasticity (Luscher C and Malenka RC, 2012). NMDA receptors are found in virtually every region of the brain (Hansen KB et al., 2017); these receptors are most dense in the hippocampus, cerebral cortex, and striatum in mice (Cotman C and Monaghan D, 1989). NMDA receptors containing the 2A subunit (GluN2A) have a higher open channel probability, faster deactivation rate, and lower GluN1/GluN2 agonist potency (Wyllie DJ et al., 2013). At birth, the presence of GluN2A containing NMDARs is low. However, as the brain develops, GluN2B-subunit containing NMDARs slowly decrease in number, concomitantly with an increase in GluN2A-subunit

containing NMDARs (Liu XB et al., 2004). A visual representation of this spatio-temporal expression of GluN2A and GluN2B in a rodent is shown in Figure 1. In mice, this 2B to 2A “switch” occurs during the first 2-5 weeks of life (McKay S et al., 2018). By adulthood, GluN2A-containing NMDARs are primarily found in the hippocampus and cortex. Similarly, GluN2B is primarily found in the hippocampus by adulthood, however GluN2B expression is lower in the cortex. This switch is thought to underpin the differing memory abilities of adolescent versus adult mice and rats, given the different kinetics each subunit provides its containing NMDA receptor (Ge M et al., 2019).

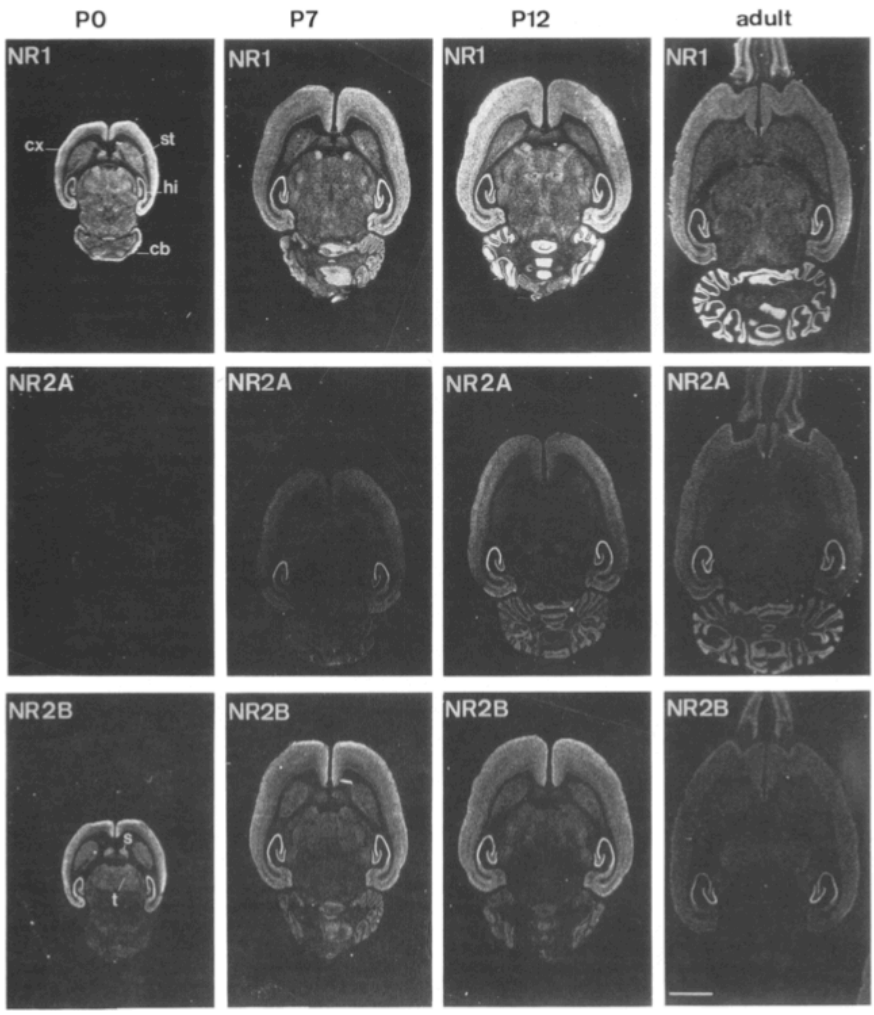

Figure 1: Spatio-temporal distribution of N1, N2A, and N2B-containing NMDARs in the post-natal rat brain. Obtained using x-ray film radiography. Scale bar represents 3.4 mm. cb: cerebellum; cx: cortex; hi: hippocampus; s: septum; st: striatum; t: thalamus. Reused with permission from Monyer et *al.* (1994).

GRIN2A **Variants**

In humans, the genetic sequence of the NMDA receptor is highly conserved; variants of all subunits are exceedingly rare. Remarkably, of the known pathogenic NMDA subunit variants, 47% (411/873) are associated with mutations in the GluN2A subunit. Figure 2 shows the distribution of various diseases by pathogenic variant for each subunit.

	EPI	ID	ASD	ADHD	MD	SCZ/BP	Total
GRIN1	25	35	4	0	20	3	85
GRIN2A	198	184	19	5	27	5	297
GRIN2B	99	185	33	2	10	5	252
GRIN2C	1	4	8	0	0	7	19
GRIN2D	12	12	5	0	0	8	26
GRIN3A	0	1	5	0	0	4	13
GRIN3B	0	0	2	0	4	2	8

Figure 2: Table of disease category for known pathogenic variants for each NMDA subunit. EPI: epilepsy; ID: intellectual disability; ASD: autism spectrum disorder; ADHD: attention-deficit hyperactivity disorder; SCZ: schizophrenia. Adapted from Yuan et *al.* (2015) and XiangWei et *al.* (2018). Data compiled from the literature and ClinVar, then cross-checked with gnomAD.

The GluN2A subunit is encoded by the *GRIN2A* gene in humans. Variants of this subunit are rare and can lead to severe disorders. Mutations in the *GRIN2A* gene have been linked to a wide variety of neurological and psychological disorders including autism, intellectual disability, aphasia, schizophrenia, and epilepsy. Figure 3 shows the distribution of gain-of-function and loss-of-function mutations found in three different *GRIN2A*-associated disorders. The data demonstrate that loss-of-function mutations are more common than gain-of-function mutations in *GRIN2A*-associated conditions.

Overall, 71% (75/106) of pathogenic known *GRIN2A* variants are loss-of-function (from Supplementary Table S1).

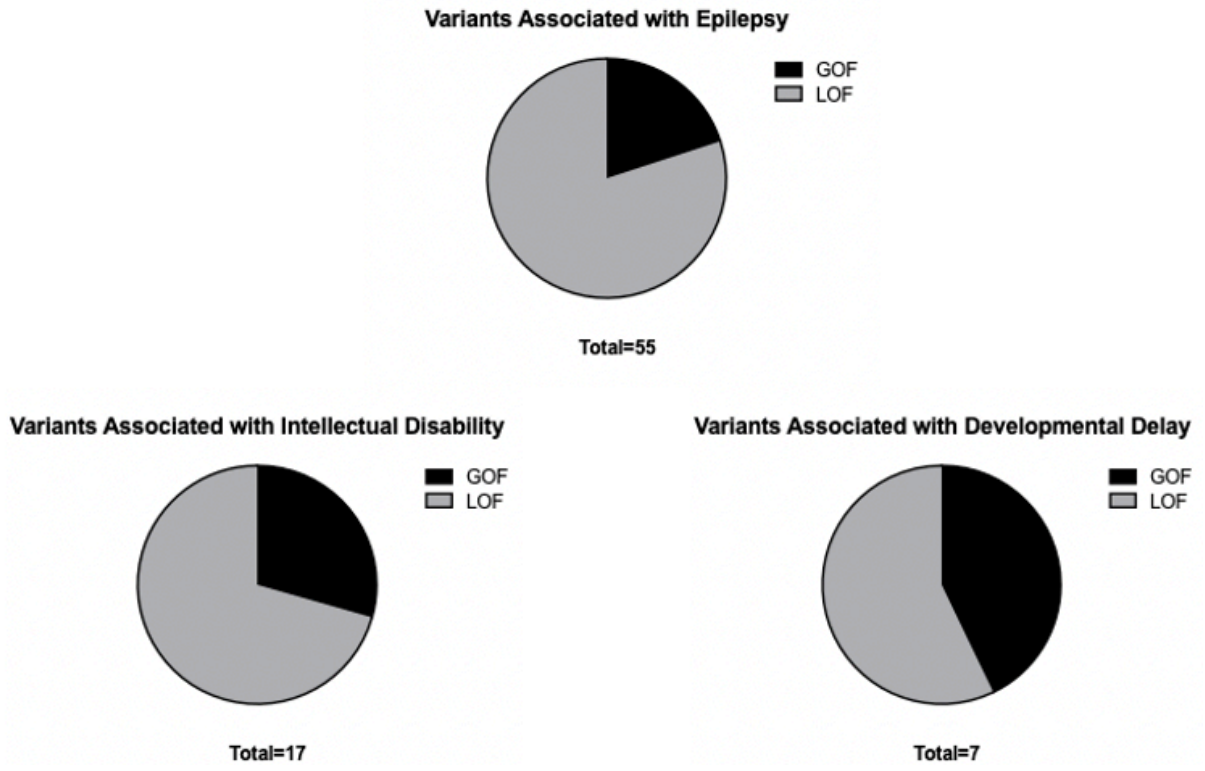

Figure 3: Frequency of distinct gain-of-function (GOF) and loss-of-function (LOF) known *GRIN2A* variant-associated disorders in humans. Composed from data contained in Supplementary Table S1, which contains information from the literature, the Center for Functional Evaluation of Rare Variants (CFERV), ClinVar, and is then cross-checked with gnomAD.

***GRIN2A*-Associated Epilepsy**

Notably, of the known *GRIN2A* variants associated with some form of epilepsy, 44 out of 55 (80%) are loss-of-function mutations (from Supplementary Table S1). It would be expected that the loss of a subunit of an excitatory receptor would not be associated with a disease that is primarily characterized by excessive excitatory firing. *GRIN2A*-associated epilepsy tends to have an age of onset around 3-6 years of age in humans (Myers KA and Scheffer IE, 1993). It is known that the 2A/2B switch also

occurs in humans. However, the timeline of this subunit switch is far less certain than that of rodents (Bar-Shira O et al., 2015). Figure 4 provides a post-mortem analysis of human subunit composition in the hippocampus.

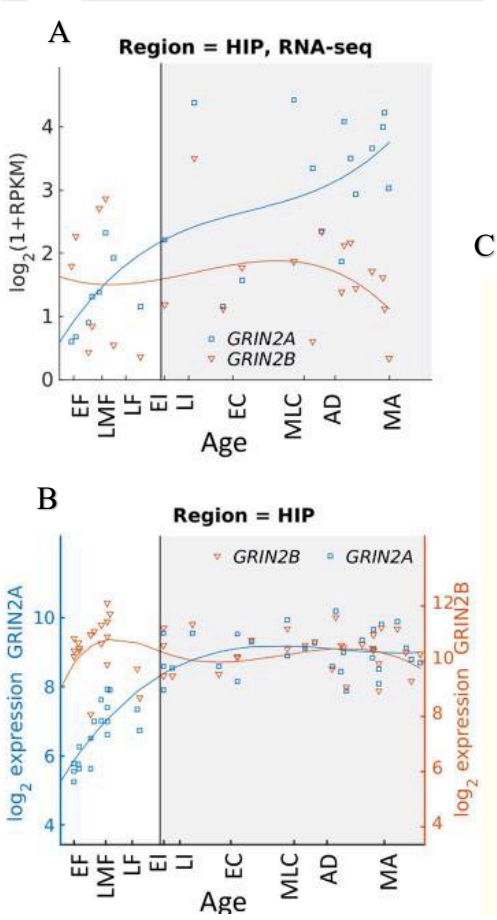

C

Donors age groups following [32].

Age group	Description	Age
EF3	Early fetal	10 PCW ≤ Age < 13 PCW
EMF4	Early-mid fetal	13 PCW ≤ Age < 16 PCW
EMF5	Early-mid fetal	16 PCW ≤ Age < 19 PCW
LMF6	Late-mid fetal	19 PCW ≤ Age < 24 PCW
LF7	Late fetal	24 PCW ≤ Age <38 PCW
EI8	Neonatal and early infancy	0 M (birth) ≤ Age <6M
LI9	Late infancy	6 M ≤ Age < 12 M
EC10	Early childhood	1 Y ≤ Age <6 Y
MLC11	Middle and late childhood	6 Y ≤ Age < 12 Y
Adol12	Adolescence	12 Y ≤ Age < 20 Y
YA13	Young adulthood	20 Y ≤ Age < 40 Y
MA14	Middle adulthood	40 Y ≤ Age < 60 Y
LA15	Late adulthood	60 Y ≤ Age

Figure 4: Post-mortem (A): RNA-sequencing; on y-axis, RPKM is reads per kilobase per million (B): microarray of GluN2A and GluN2B in human hippocampus. (C): Abbreviations for each stage of life indicated on x-axes. Adapted from Bar-Shira et *al*. (PLoS Computational Biology, 2015) under the terms of the Creative Commons Attribution License.

With the limited data available, it appears as though the onset of *GRIN2A*-related epilepsies may occur around the time when a change in subunit composition is expected to occur in humans. Loss-of-function (LOF) *GRIN2A* mutations are also

112 associated with other disorders such as learning disabilities, intellectual disabilities, and
113 developmental delay, as is shown in Figure 5.

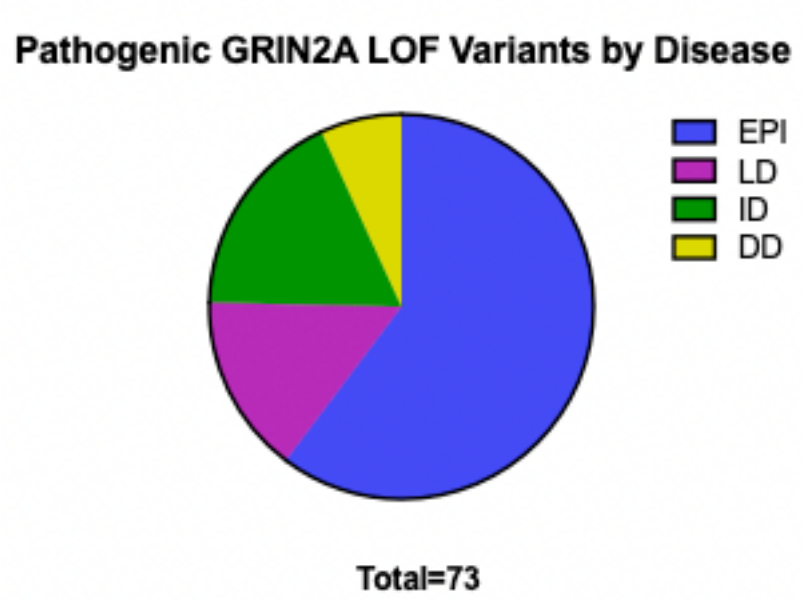

114

115 Figure 5: Frequency of various disorders for pathogenic loss-of-function *GRIN2A*
116 variants. EPI: epilepsy; LD: language disability; ID: intellectual disability; DD:
117 developmental delay. Composed from data contained in Supplementary Table S1 which
118 contains information from the literature, the Center for Functional Evaluation of Rare
119 Variants (CFERV), ClinVar, and is cross-checked with gnomAD.
120
121 **Neuroinflammation in Epilepsy**

122 Although primarily a disease of hyperexcitability, there is a neuroinflammatory
123 response associated with status epilepticus (SE) and seizures. Status epilepticus is
124 defined as a seizure lasting more than 5 minutes continuously, or as two or more
125 seizures within 5 minutes where there is incomplete recovery of consciousness between
126 seizures (Trinka E et al., 2015). The neuroinflammation that follows SE worsens
127 epileptogenesis (the process by which a brain is converted from normal to epileptic).
128 The subsequent neuroinflammation further enhances neuronal cell loss,
129 hyperexcitability, and the changes in synaptic plasticity that follows SE (Rana A and

Musto AE, 2018). Though the mechanisms of this neuroinflammation are not yet fully elucidated, they appear to involve damaged neurons signaling to nearby astrocytes and microglia (de Lanerolle NC et al., 2010; Hiragi T et al., 2018). The astrocytes and microglia then release cytokines and chemokines that weaken the blood-brain barrier and permit peripheral monocytes and lymphocytes to enter the brain (Keaney J and Campbell M, 2015). It is unclear whether the actions of microglia subsequent to status epilepticus, such as their role in neurogenesis and synaptic pruning, leads to a net neuroprotective or neurodegenerative effect (Andoh M et al., 2019). Notably, treatment with cyclooxygenase-2 inhibitors, prostaglandin receptor antagonists, and cytokine receptor antagonists appear to decrease inflammation and prevent the breakdown of the blood-brain barrier that when administered after SE in some mouse models (Vezzani A et al., 2015). These anti-inflammatory actions can lead to a neuroprotective effect in these models; this neuroprotective effect of anti-inflammatory agents is due in part to prevention of neuronal cell loss and hyperexcitability (Dey A et al., 2016). Finally, epidemiological data show that inhibition of cyclooxygenase may prevent epilepsy; use of NSAIDs over long periods in rheumatoid arthritis patients is associated with a lower incidence of epilepsy in that population (Chang KH et al., 2015).

GluN2A and Neuroinflammation

Changes to the GluN2A subunit can have complex, wide-ranging consequences. Previous studies have established a clear involvement of the GluN2A-containing NMDA receptor in the process of neuroinflammation. Mice lacking the GluN2A subunit (*Grin2a* KO mice) are resistant to tonic inflammatory pain (Hizue M et al., 2005). *Grin2a* KO

mice have also been shown to suffer from redox dysregulation in adolescence that can lead to neuroinflammatory consequences in adulthood. Oxidative insults in adolescent *Grin2a* KO mice can lead to persistent microglial activation in adulthood (Cardis R et al., 2018). Furthermore, unpublished data from our lab in collaboration with others find that *Grin2a* KO mice are far more susceptible to febrile seizures. Conversely, *Grin2a* KO mice also have a largely attenuated neuroinflammatory response to lipopolysaccharide (LPS) injections, and do not suffer from any depression as a result of LPS, unlike wild-type controls (Francija E et al., 2019). Additionally, the processes of microglia from *Grin2a* KO mice are unable to converge on damaged neurons in some brain regions (Eyo UB et al., 2018). Therefore, in *Grin2a* knockout mice, there appears to be a general resistance to neuroinflammation combined with instances where there is greater susceptibility to unregulated neuroinflammation. Before examining the mechanism, however, the basic premise of this theory must be tested. In order to establish this "theory of inflammatory instability," baseline levels of neuroinflammation must first be determined in mice lacking the GluN2A subunit.

Interestingly, there are multiple documented cases of human patients with *GRIN2A*-associated epilepsy responding well to immunotherapies such as intravenous immunoglobulin (IVIG) and corticosteroids. These patients display normal brain activity via electroencephalogram (EEG) recordings, improved language, and improved sleep architecture in response to these immunotherapies (Hausman-Kedem M et al., 2020). A *GRIN2A*-associated epilepsy patient's EEG response to this type of therapy is shown in Figure 6. Corticosteroids are a well-known anti-inflammatory treatment used in a wide variety of inflammatory conditions. These medications work by directly affecting the

transcription of a number of different pro-inflammatory genes (Barnes PJ, 2006). The mechanism of action for IVIG is less well-understood but appears to involve changes in cytokine levels as well as a decrease in certain pro-inflammatory autoantibodies (Billiau AD et al., 2007).

A

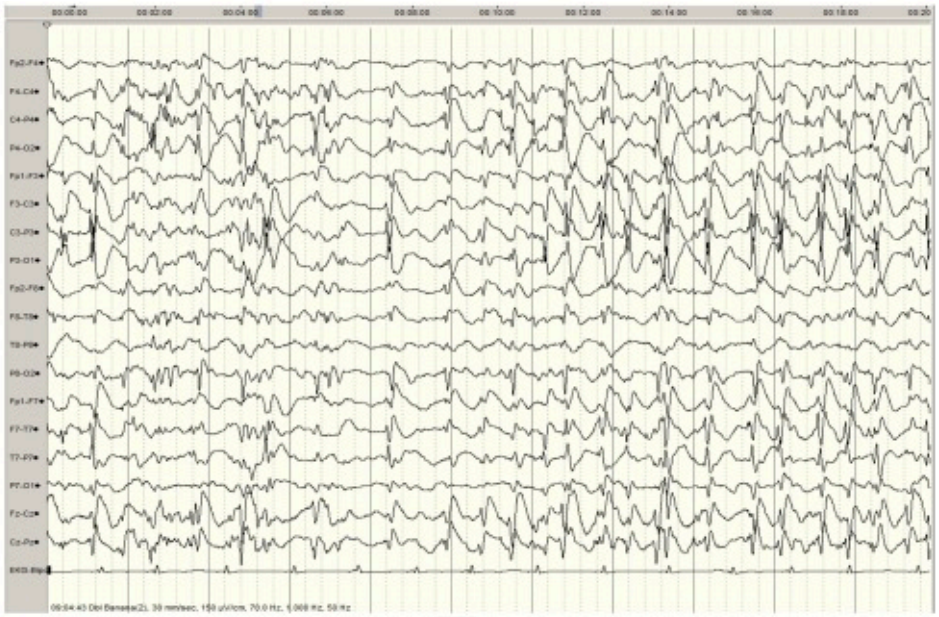

B

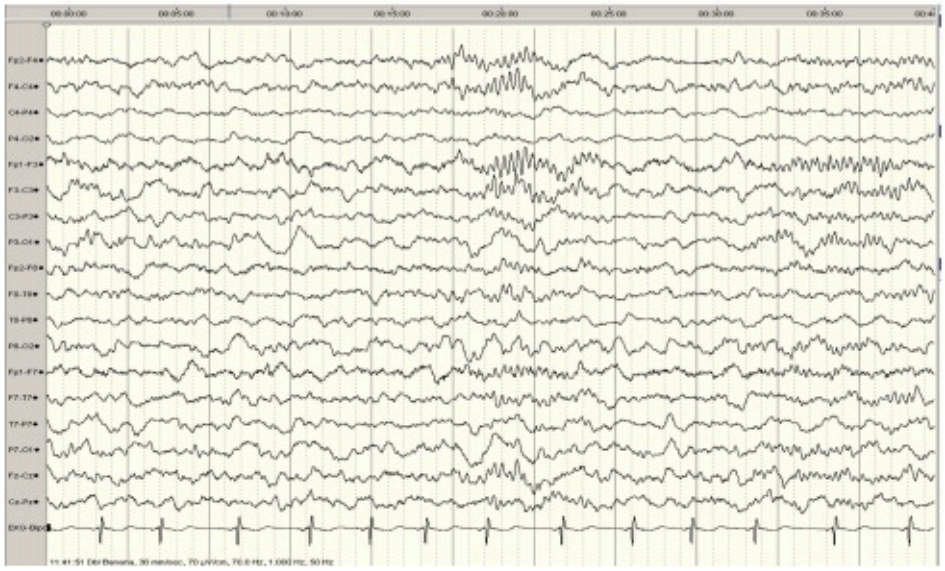

Figure 6: EEG recording of a GRIN2A loss-of-function mutation patient before (A) and after (B) intravenous immunoglobulin treatment, an anti-inflammatory therapy. Reused from Hasuman-Keddem et *al*. (Epilepsy Research, 2020) with permission.

Microglia and Astrocytes in Neuroinflammation

Microglia are the resident immune system of the central nervous system (CNS) (van Rossum D and Hanisch UK, 2004). These cells survey the CNS for pathogens and unnecessary neurons and synapses. In their surveilling role, microglia assume the "rested" state with a stationary cell body and thin processes. When microglia encounter pathogens and brain tissue damage, their morphology can rapidly change into the "active" state with a more ameboid shape as the processes contract closer to the cell body and are thicker. Microglia can also respond in this way to various factors that can be released by nearby neurons, such as cytokines, necrosis factors, and potassium. The microglia can then engulf the offending matter via phagocytosis (Perry VH et al., 2010) or initiate a neuroinflammatory cascade (Harry GJ and Kraft AD, 2008). Part of this cascade is the infiltration of peripheral immune cells as mentioned earlier. In this process, the genes expressed by the microglia, as well as the degree to which they are expressed, changes markedly (Holtman IR et al., 2015). Thus, microglial activation is crucial to neuroinflammation.

Astrocytes are also a type of glial cell present in the brain. These star-shaped cells perform a wide variety of functions. They are mostly known for their function in regulating the extracellular environment directly around neurons. Astrocyte processes are present at virtually every synapse; at the synapse, astrocytes maintain pH, ion gradients, and neurotransmitter concentrations of the area immediately surrounding the neurons. These actions are necessary for neurons to function correctly. Additionally, GABA, glycine, and glutamate are taken up by astrocytes to be recycled after neuronal firing. Other functions of astrocytes include regulating blood flow to the CNS via

attachment and direct signaling to cells of the blood-brain barrier (Abbott NJ et al., 2006). Astrocytes also appear to play a role in synaptic plasticity via direct release of neurotransmitters, as well as the release of growth factors that influence the neurons of the synapse. Astrocytes may also be involved in synaptic pruning by tagging synapses for destruction (Sofroniew MV and Vinters HV, 2010). Finally, astrocytes play an integral role in controlling brain damage by migrating to damaged parts of the brain and act to fill in gaps left by dead neurons. In doing so, they provide structural support for the brain and are integral to the scarring process (Stichel CC and Muller HW, 1998).

During the neuroinflammatory process microglia and astrocytes undergo morphological changes called gliosis; in this state, both cell types release proinflammatory cytokines and reactive oxygen species to propagate inflammatory signaling and induce neuronal death. Cytokines released from both microglia and astrocytes can signal cells of both types, leading to reciprocal activation between cell types (Matejuk A and Ransohoff RM, 2020). During gliosis, the expression of many genes change dramatically in both these cell types (Pekny M and Pekna M, 2016). Activation of microglia and astrocytes has been implicated in the neuroinflammation that is associated with a wide variety of neurological diseases, including epilepsy (Kwon HS and Koh SH, 2020). In microglia one such gene is *AIF1* (Allograft Inflammatory Factor 1), which codes for ionized calcium-binding adapter molecule 1 (IBA1). IBA1 is a calcium-binding protein which is part of a signaling cascade leading to membrane ruffling and phagocytosis in cells that express it. In the CNS under normal conditions, the only cells that express this protein are microglia (Ohsawa K et al., 2000). Measuring

baseline expression of this protein is thus an indicator of the degree of microglial activation in the CNS. In astrocytes, the *GFAP* gene encodes the Glial Fibrillary Acidic Protein (GFAP). This protein is an intermediate filament and contributes to the structure of the astrocyte. Notably, this protein is more highly expressed in reactive astrocytes; when astrocytes become activated, the expression of this protein helps move the cell processes away from the soma and into the characteristic star-like shape of a reactive astrocyte. Given that only astrocytes express GFAP in the areas of the CNS that lack neural stem cells, staining for GFAP can therefore demonstrate the degree of astrocyte reactivity in the CNS (Eng LF et al., 2000; Mamber C et al., 2012). By determining the activation state of microglia and astrocytes, an overall measure of the level of neuroinflammation at baseline can be obtained. Interestingly, NMDA receptors are found in astrocytes and microglia. In astrocytes, modification of NMDARs appears to change astrocyte homeostasis (Skowronska K et al., 2019). Activation of microglial NMDA receptors leads to their proliferation and activation (Raghunatha P et al., 2020).

Rationale

Though previous studies have examined neuroinflammation in the *Grin2a* KO mouse model under various conditions, none have reported baseline neuroinflammation levels. Given the combination of resistance to LPS-induced neuroinflammation, combined with instances of enhanced neuroinflammatory susceptibility such as a greater incidence of febrile seizures and persistent microglial activation after oxidative damage, establishing any difference in baseline neuroinflammation is thus important for understanding the effects of *Grin2a* knockout on neuroinflammation after injury and

during disease (Cardis R, Cabungcal JH, Dwir D, Do KQ and Steullet P, 2018; Francija E, Petrovic Z, Brkic Z, Mitic M, Radulovic J and Adzic M, 2019). Though there are multiple markers for neuroinflammation, the one commonality of this biological process in many diseases that create neuroinflammation is the activation of microglia and astrocytes. Therefore, by using immunohistochemistry, the fluorescence of microglia expressing IBA1 and astrocytes expressing GFAP will be measured. By determining the area of fluorescence for these proteins in wild-type and *Grin2a* KO mice, basal levels of neuroinflammation (i.e. neuroinflammation without any prior insult) can be determined

Hypothesis

The proposed “theory of inflammatory instability” to describe the *Grin2a* KO mice is composed of two parts: a lower basal level of neuroinflammation and an exaggerated response to certain insults. Therefore, at baseline, it is hypothesized that *Grin2a* KO mice will display lower GFAP and IBA1 fluorescence area compared to wild-type controls.

Materials and Methods

Mice

All mice were bred and procedures conducted at Emory University, which is fully accredited by the Association for Assessment and Accreditation of Laboratory Care. All procedures were Institutional Animal Care and Use Committee approved and performed in accordance with state and federal Animal Welfare Acts and Public Health Service policies. *Grin2a* knockout mice (Sakimura K et al., 1995) were back-crossed onto a

C57BL6/J background for over 20 generations. These mice contain a sequence upstream of the *Grin2a* gene that disrupts transcription of the gene. *Grin2a* transcript and GluN2A protein is not detected in Grin2a KO mice (Sakimura K et al., 1995). Wild type and knockout mice were bred in-house and stored on the same rack to minimize assay differences due to stress level. All mice were kept in a maximum of 5 per cage, on a 12-hour light/dark cycle. Food and water were provided *ad libitum*.

Tissue harvesting

Adolescent postnatal day (P) 20-25 and adult P 80-120 mice were sacrificed using deep isoflurane anesthesia. Lack of consciousness was confirmed using loss of righting reflex and absence of response after toe pinch. Mice were then perfused first with 1X PBS followed by 4% paraformaldehyde (PFA). After harvesting, brains were placed in 4% PFA overnight. Brains were then placed in 30% sucrose (w/v) until they sank then 50-um thick coronal sections were obtained using a cryostat (Leica). Coronal sections were obtained through the entire hippocampus, from dorsal to ventral, with each replicate consisting of 5-6 sections spaced roughly 250 μm apart. Sections were then stored in 1X PBS at 4°C until used.

IBA1 and GFAP Staining

The staining procedure for IBA1 and GFAP was adapted from (McLeod F et al., 2017). A blocking buffer was made consisting of 1X PBS supplemented with 15% normal goat serum (NGS, Abcam ab7481), 1% bovine serum albumin (BSA, Jackson Immuno) and 0.5% Triton-X 100. Sections were first incubated in blocking buffer for 3.5 hours at room

temperature, before being transferred to blocking buffer containing either GFAP (1:3000, Abcam ab7260) or IBA1 (1:1500, Abcam ab178846) and left to incubate overnight at 4°C. Next, sections were washed three times in 1X PBS buffer before being placed in blocking buffer containing AlexaFluor 488®- (1:500, Abcam ab150077) for 3 hours at room temperature. After three more washes in 1X PBS, sections were incubated for 20 minutes with DAPI solution (2 uM). Sections were mounted and coverslipped using #1.5 coverslips with hard-setting Prolong Gold® Antifade (ThermoFisher) as the mounting medium.

Imaging and Analysis

Images were obtained using a Nikon ECLIPSE Ti2 line-scanning confocal microscope with a Nikon A1R HD 25 camera. Z-stacks were taken by positioning the focal plane to the top of the section and imaging a range of 3.6 μm with a step size of 0.4 μm; in the IBA1 images obtained from sections taken from adolescent mice, the stack settings were slightly different. In these slices, the focal plane was moved to the middle of the sections and images taken with a step size of 1.1 μm and a range of 11 μm. Images were taken of the *cornu ammonis 1* (CA1) at 20X objective magnification using NYQUIST zoom. A single z-stack was taken in CA1 of the hippocampus of each section, with 4-6 sections per mouse. The side of the hippocampus imaged alternated left and right between sections. Analysis was performed using ImageJ version 2.1.0/1.53c (National Institutes of Health). In order to perform the analysis, z-stacks were z-projected with maximum intensity to create a single image out of the stack images; the fractional area of fluorescence was determined by creating a binary

intensity threshold and fractionating the image into area of pixels above the threshold divided by total image area. The average of this fractional area from the 4-6 sections per mouse was plotted as each data point. A visual representation of the z-projection and intensity thresholding is shown in Figure 7.

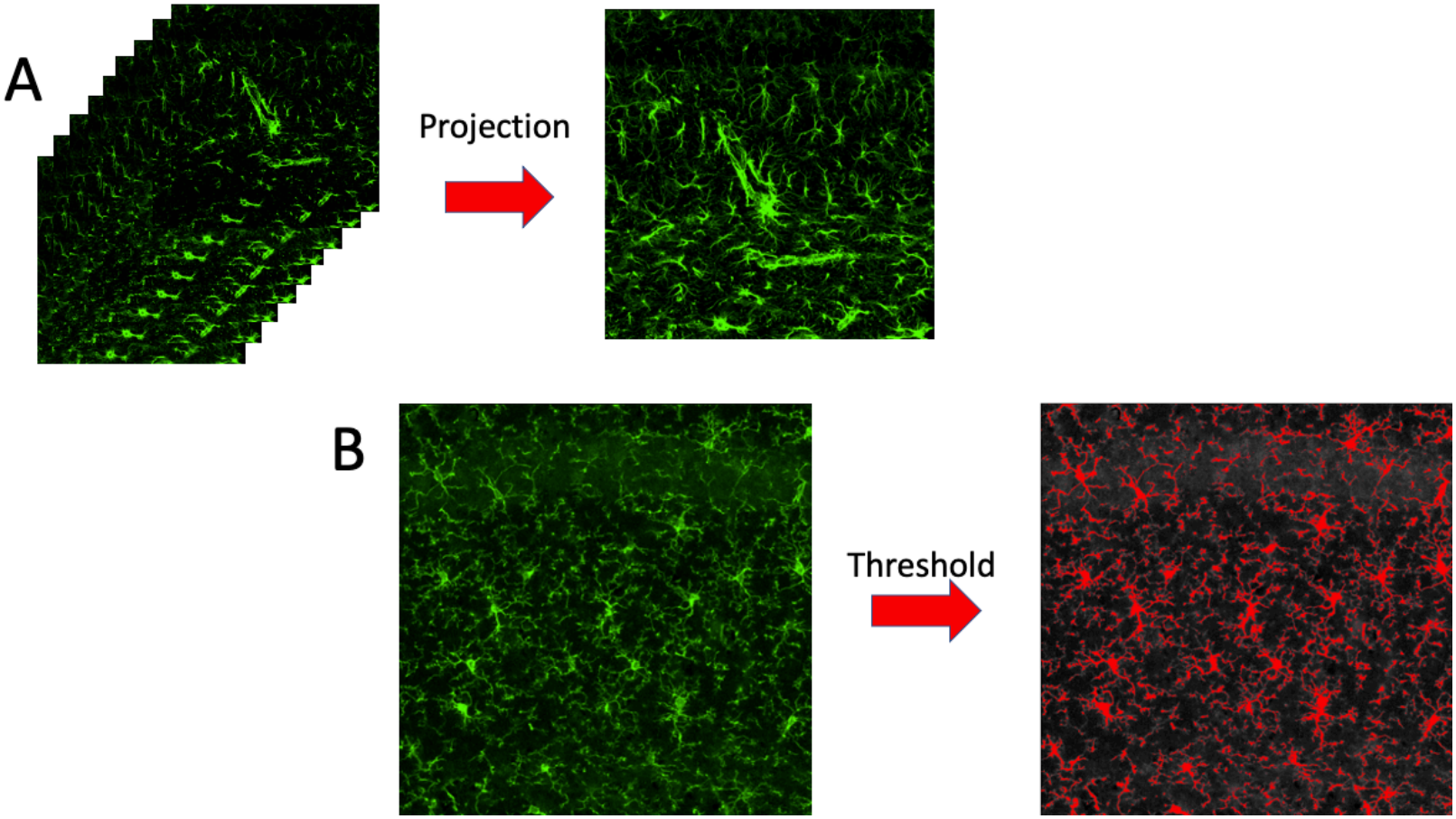

Figure 7: Representation of image stack projecting and thresholding. (A): Z-projection of 9 individual component sample GFAP images of z-stack (B): Binary intensity thresholding of sample z-projected IBA1 image.

Statistical Analysis

Statistical analysis was performed using GraphPad Prism 9.0.0 (GraphPad Software) and Excel version 16.47 (Microsoft). The data were first tested for outliers using the Grubbs' test. Then, the variances between data sets were tested for similarity

using an F-test, with α=.05 (two-tailed). Finally, data sets were tested for normality using both the Shapiro-Wilk test, as well as the Kolmogorov-Smirnov test. Data sets were then compared to each other using a two-tailed *t*-test.

Results

Given the high prevalence of temporal lobe epilepsy in humans (including *GRIN2A*-associated epilepsy patients) (Gao K et al., 2017), the high density of NMDA receptors (including GluN2A) in the hippocampus (Petralia RS et al., 1994), as well as the wealth of literature demonstrating hippocampal gliosis and neuronal cell loss that occurs in temporal lobe epilepsy (Al Sufiani F and Ang LC, 2012), we chose to investigate neuroinflammation in the hippocampus using immunohistochemistry. Images were taken at the CA1 radiatum area of the hippocampus, oriented with the pyramidale layer at the top of each image. The radiatum consists of CA1 apical dendrites that receive axonal input from the CA3 pyramidal cells (Harris KM and Weinberg RJ, 2012).

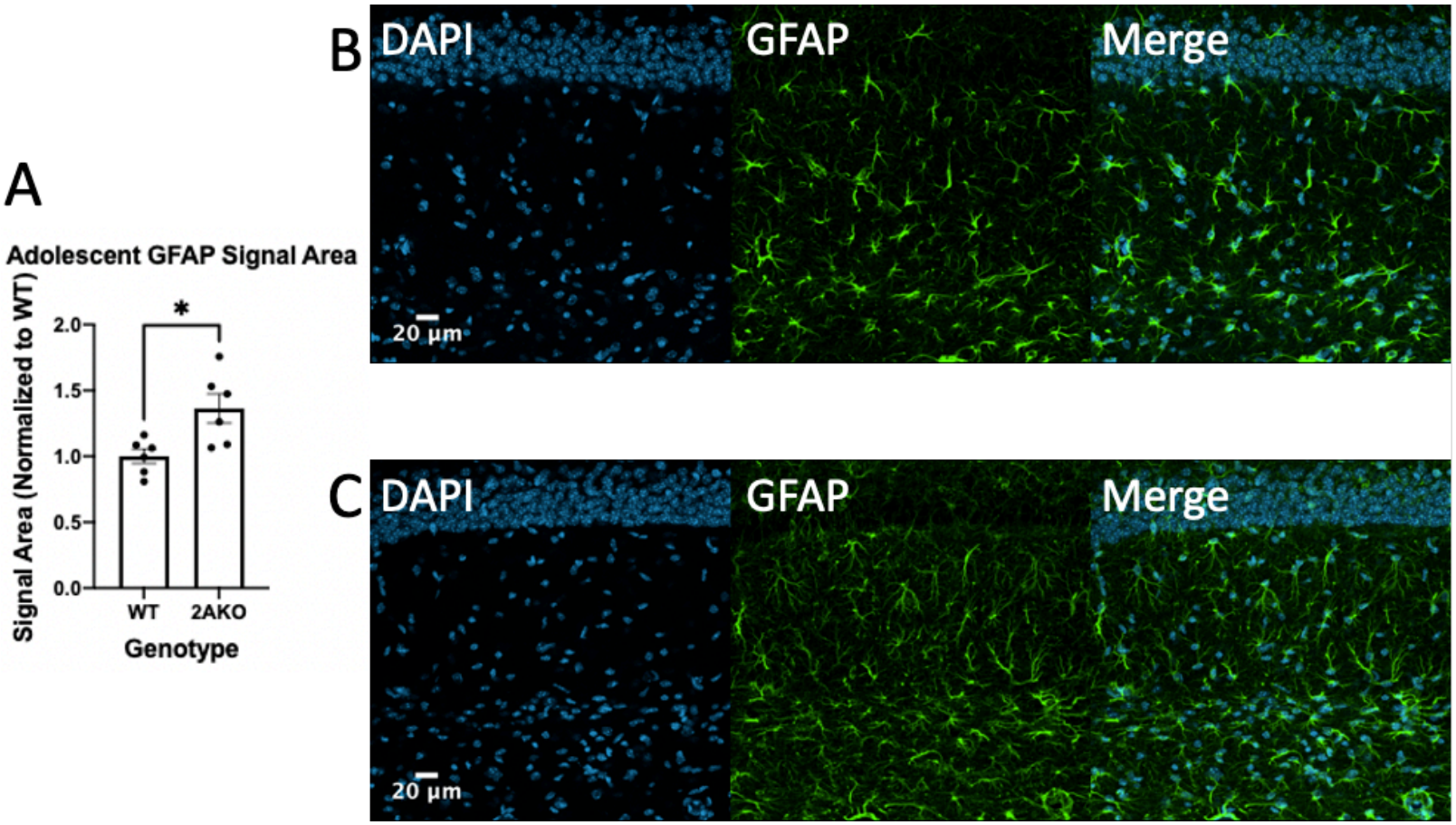

Figure 8: **Adolescent *Grin2a* KO mice have a greater average area of GFAP fluorescence compared to wild-type controls.** (A): Adolescent (P20-25) GFAP signal area by genotype, normalized to the wild-type average. Each data point represents one mouse, which is composed of 4-6 sections. Data points are composed of three males and three females per genotype. Asterisk indicates statistical significance after performing two-tailed t-test (p=.0146). Bars represent the mean, and error bars represent standard error of the mean (SEM). (B): Representative DAPI/GFAP/Merge image in CA1 radiatum of WT mouse (C): Representative DAPI/GFAP/Merge image in CA1 radiatum of *Grin2a* KO mouse. Scale bars represent 20µm.

Interestingly, the GFAP signal area in adolescents was higher in *Grin2a* KO mice versus wild-type controls as show In Figure 8. The 1.36-fold increase in signal area was found to be statistically significant after performing a two-tailed t-test (p=.0146).

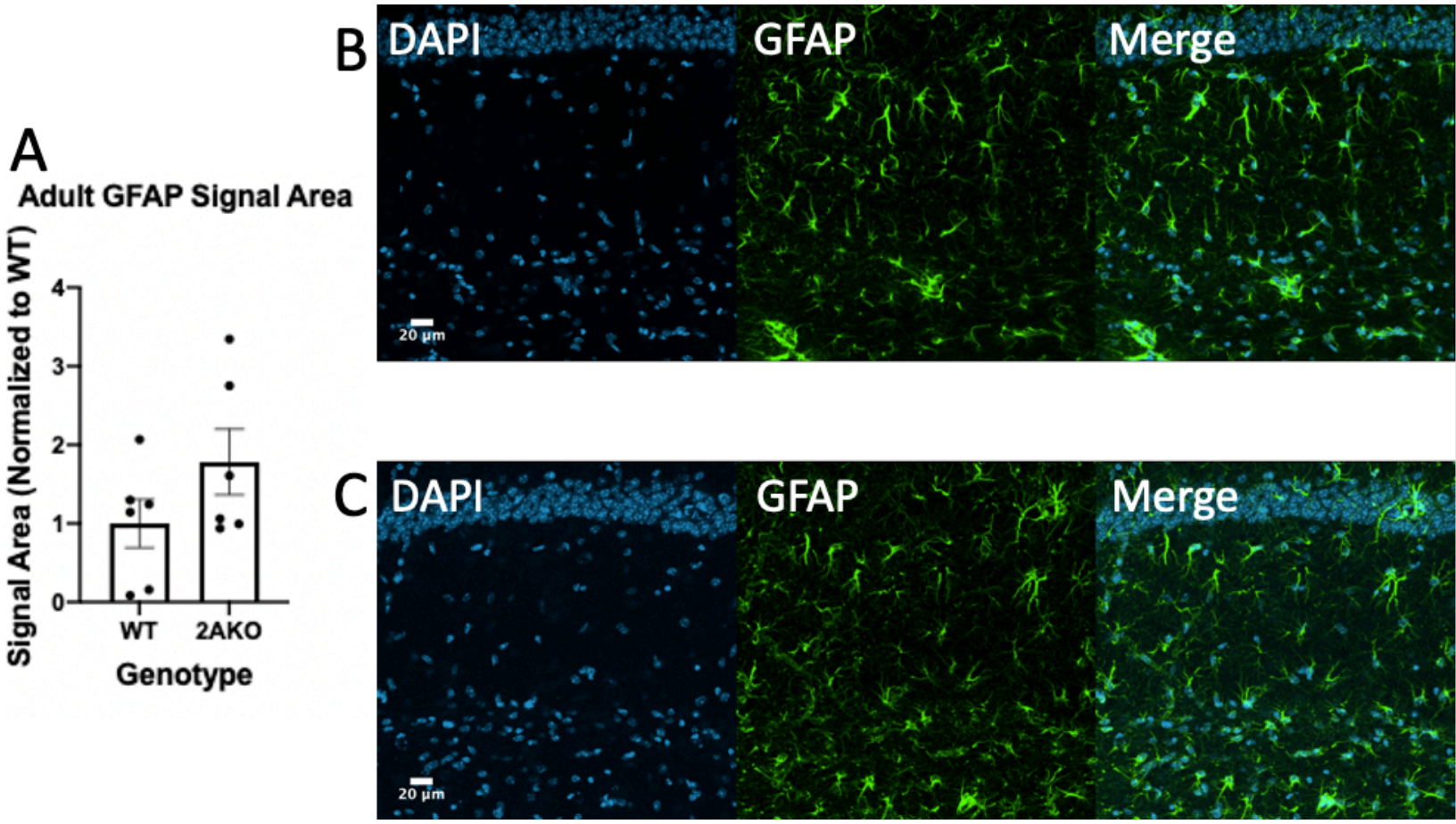

Figure 9: **No change in average GFAP fluorescence area between adult wild-type and *Grin2a* KO mice.** (A): Adult (P80-120) GFAP signal area by genotype, normalized to the wild-type average. Each data point represents one mouse, which is composed of 4-6 sections. Data points are composed of three males and three females per genotype. The difference between genotypes was not statistically significant (p=.1632, two-tailed). Bars represent the mean, and error bars represent standard error of the mean (SEM). (B): Representative DAPI/GFAP/Merge image in CA1 radiatum of WT mouse (C): Representative DAPI/GFAP/Merge image in CA1 radiatum of *Grin2a* KO mouse. Scale bars represent 20µm.

In adults, no significant difference was found between WT and *Grin2a* KO GFAP staining according to Figure 9 (p=.1632, two-tailed). This data set had a far higher

variability than the adolescent GFAP data set. The representative image of the *Grin2a* KO mouse (Figure 9 panel C), though similar in area to the WT mouse (Figure 9 panel B), appears to have more fluorescence of primary processes.

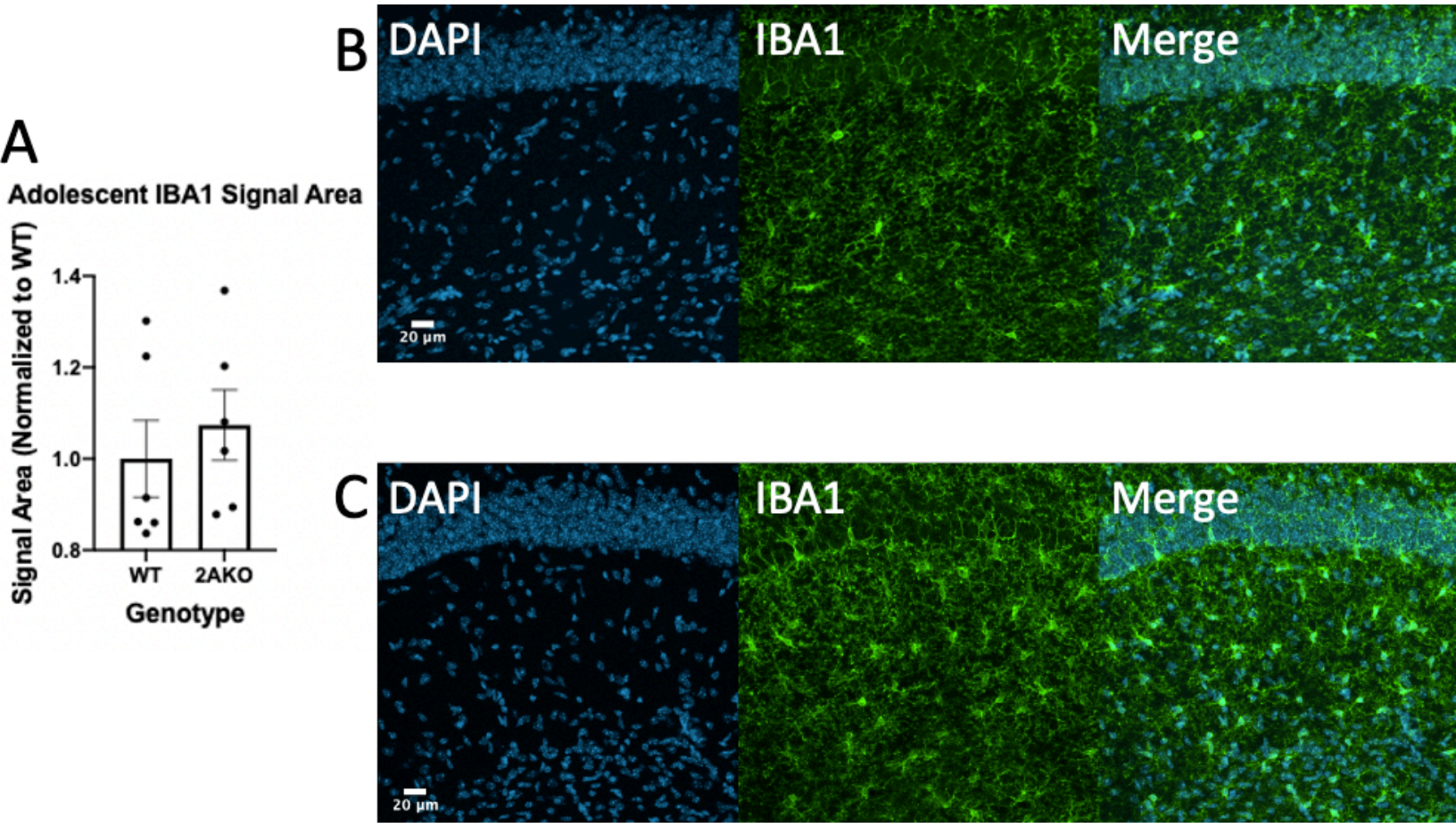

Figure 10: **No change in average IBA1 fluorescence area between adolescent wild-type and *Grin2a* KO mice.** (A): Adolescent (P20-25) IBA1 signal area by genotype, normalized to the wild-type average. Each data point represents one mouse, which is composed of 4-6 sections. Data points are composed of three males and three females per genotype. The difference between genotypes was not statistically significant (p=.5331, two-tailed). Bars represent the mean, and error bars represent standard error of the mean (SEM). (B): Representative DAPI/IBA1/Merge image in CA1 radiatum of WT mouse (C): Representative DAPI/IBA1/Merge image in CA1 radiatum of *Grin2a* KO mouse. Scale bars represent 20µm.

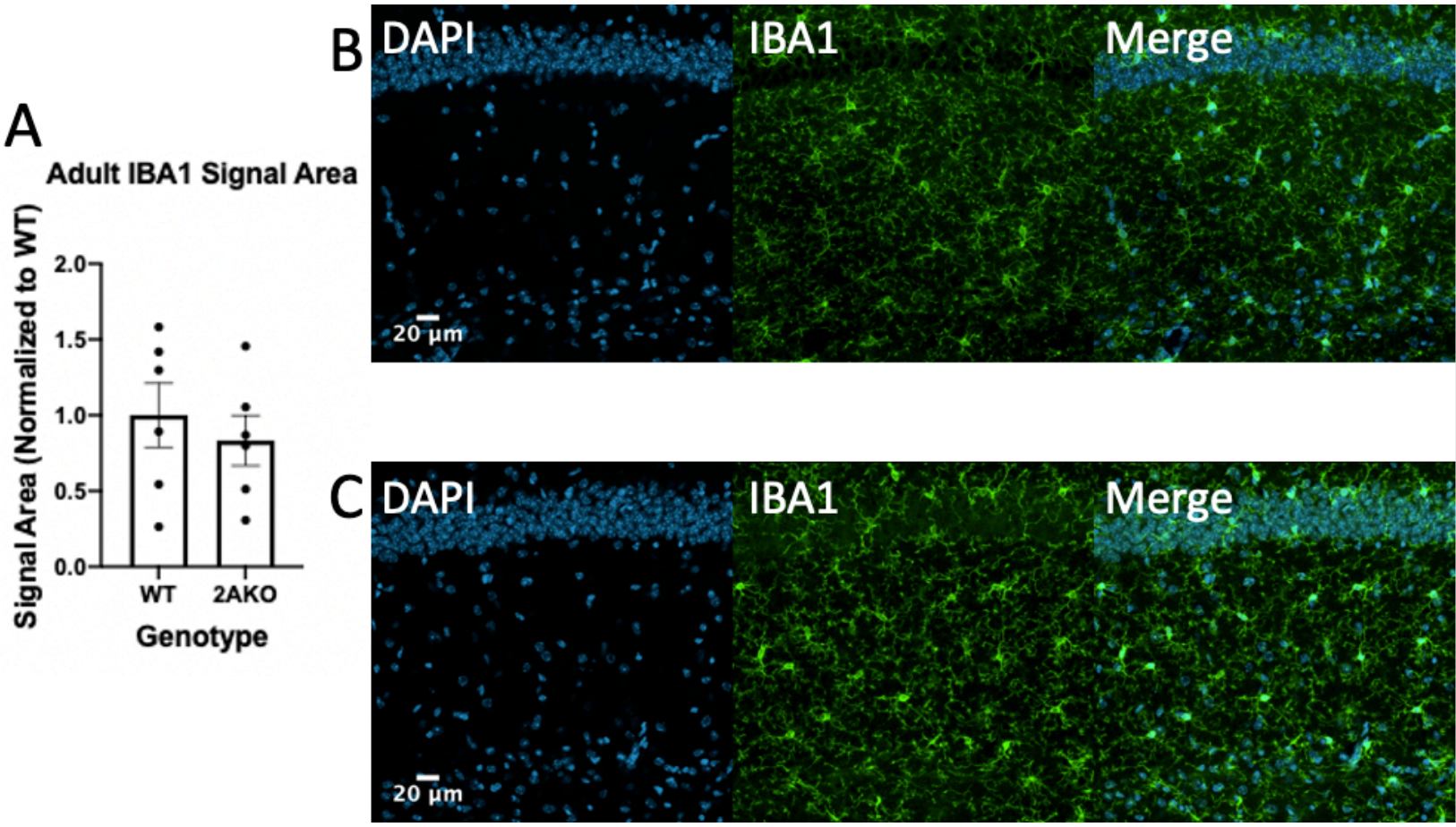

Figure 11: **No change in average IBA1 fluorescence area between adult wild-type and *Grin2a* KO mice.** (A): Adult (P80-120) IBA1 signal area by genotype, normalized to the wild-type average. Each data point represents one mouse, which is composed of 4-6 sections. Data points are composed of three males and three females per genotype. The difference between genotypes was not statistically significant (p=.5494, two-tailed). Bars represent the mean, and error bars represent standard error of the mean (SEM). (B): Representative DAPI/IBA1/Merge image in CA1 radiatum of WT mouse (C): Representative DAPI/IBA1/Merge image in CA1 radiatum of *Grin2a* KO mouse. Scale bars represent 20µm.

In both adolescents and adults, there was no significant difference in IBA1 fluorescence area (adolescent: p=.5331; adult: p=.5494, two-tailed).

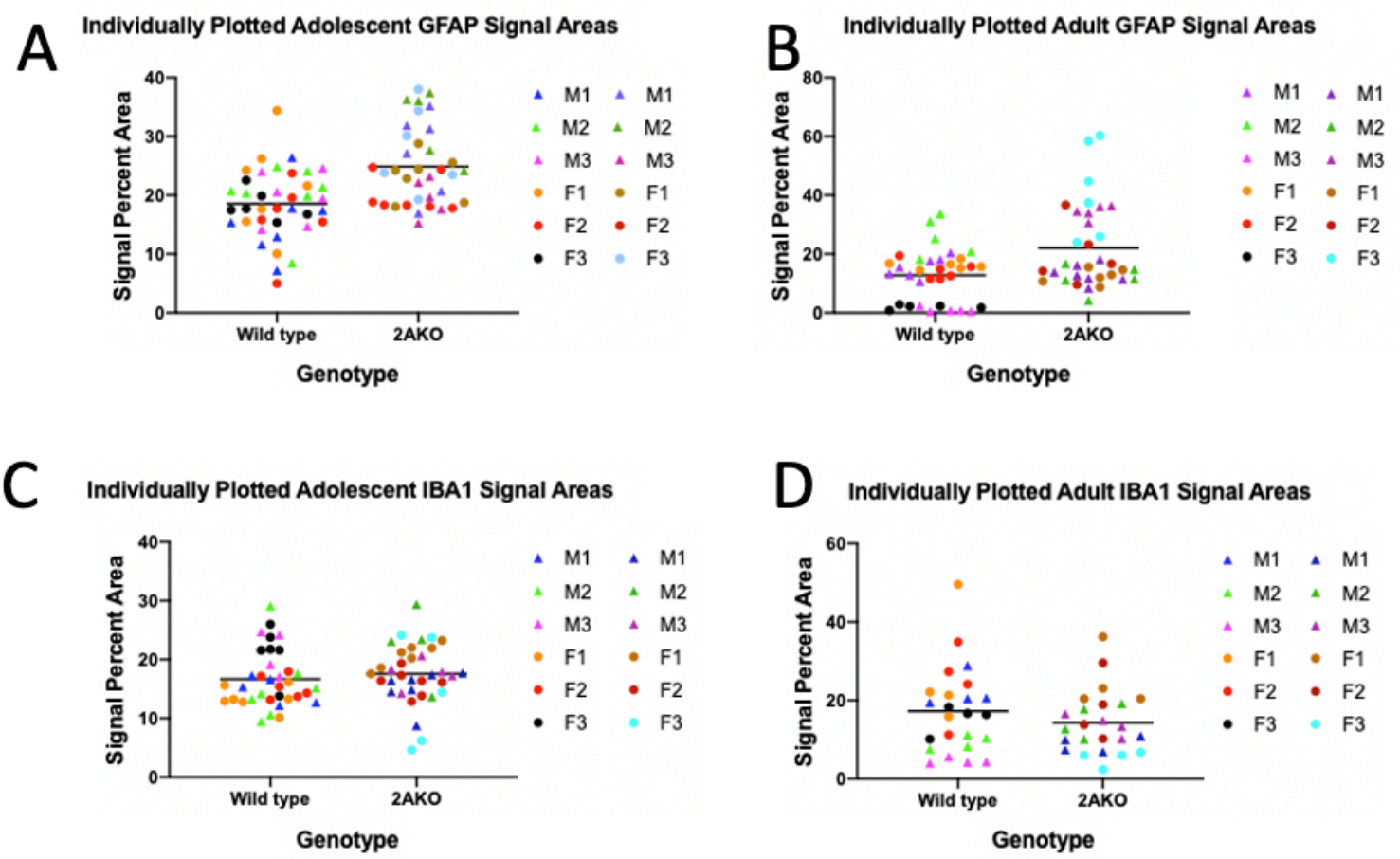

Figure 12: **Variability in signal between sections of the same mouse**. Each point represents a single 9-image z-stack (10-image stack for adolescent IBA1) in the CA1 radiatum of one section, with 4-6 sections per mouse. Points of the same color represent different stacks of the same mouse. (A): Adolescent GFAP mice (B): Adult GFAP mice (C): Adolescent IBA1 mice (D): Adult IBA1 mice. Lines represent the grand mean of all individual sections.

Figures 8-11 show plots where each mouse represents a single data point. Presenting the data in this way best addresses the question at hand, yet also masks individual section variability within each mouse. Therefore, each individual section of

each mouse was plotted for adolescent and adult GFAP/IBA1 stains (Figure 12) in order to demonstrate the degree of similarity of fluorescence signal area between each section of each mouse. Each color represents one mouse. Overall, the figure shows that most sections of each mouse were roughly comparable to each other in terms of signal area. Some mice did have noticeable variability in fluorescent area between sections, however. Most data points appear fairly close to other points of the same color, thus indicating that variability was not extreme.

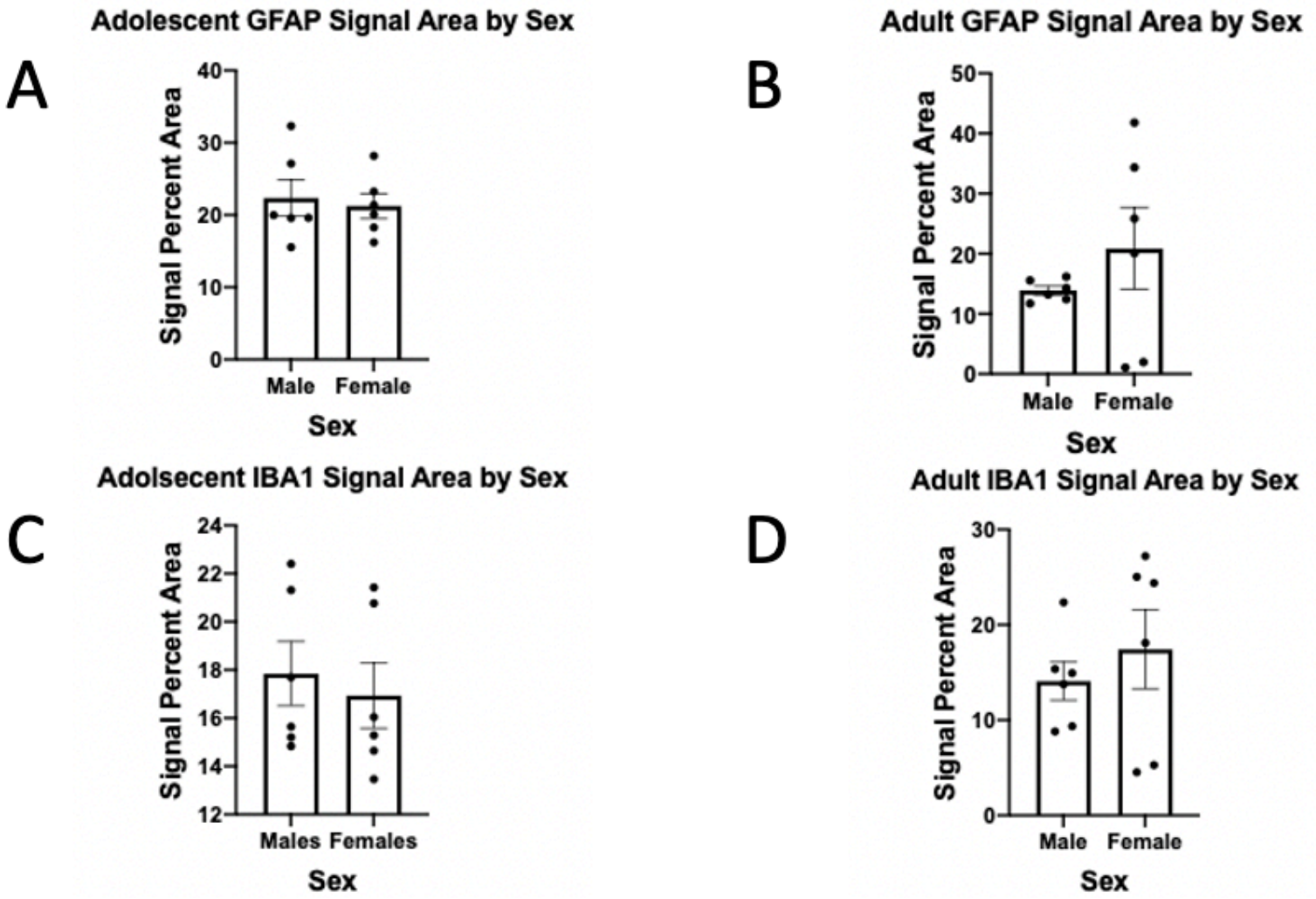

Figure 13: **No differences in fluorescent areas by sex**. Each data point represents one mouse, composed of 4-6 sections. Columns are divided by sex and represent pooled WT and *Grin2a* KO mice for each sex (3 of each genotype). (A): Adolescent GFAP (p=.6436) (B): Adult GFAP (p=.4857) (C): Adolescent IBA1 (p=.7188) (D): Adult IBA1 (p=.3344). Error bars represent standard error of the mean (SEM).

Finally, though the mice were selected so as to balance the sexes (3 mice per sex per condition), Figure 13 shows signal percent area by sex. Male and female WT and *Grin2a* KO mice were pooled together by sex in order to determine if there was a sex difference; Figure 13 clearly shows that there is no significant difference between males and females.

Overall, in both adult and adolescent mice, no significant difference could be observed between WT and *Grin2a* KO mice except for adolescent GFAP area. However, this difference is small, and caution must be taken when interpreting these results. At baseline, neuroinflammation differs only slightly between adolescent WT and *Grin2a* KO mice, and only when measured via GFAP.

Discussion

Result and Primary Conclusion

Provided that the methodological limitations are considered, the present data require that the "theory of inflammatory instability" be modified to account for these results. It was previously hypothesized that *Grin2a* KO mice would have lower neuroinflammation at baseline, with an exaggerated reaction to insult. However, the data here reject the former component of this theory. Instead, *Grin2a* KO mice have a slightly increased baseline level neuroinflammation when measured via GFAP, and only in adolescence. Therefore, all that can be concluded from the data is that in adolescence, the area covered by astrocytes in the CA1 radiatum is somewhat higher in *Grin2a* KO mice.

Relation to Previous Works

Previous work has shown that there is delayed perineuronal net development in *Grin2a* KO mice, as a result of disruption to antioxidant systems such as glutathione (Cardis R, Cabungcal JH, Dwir D, Do KQ and Steullet P, 2018). Such redox dysfunction

may also lead to transient differences in astrocyte reactivity that resolve by adulthood. Or it may be that the differences in astrocyte reactivity during development contributes to this delay in perineuronal net development. Interestingly, previous research into temporal lobe epilepsy (which is common in *GRIN2A*-associated epilepsy patients) (Carvill GL et al., 2013) consistently finds reactive astrogliosis in the hippocampus (Das A et al., 2012; Loewen JL et al., 2016; Lu J et al., 2019). The results of the current work thus provide a possible explanation for the development of *GRIN2A*-associated epilepsies. It appears as though at baseline, there is greater astrocyte reactivity. Previous research has demonstrated that reactive astrogliosis can itself create spontaneous recurrent seizures in the absence of any other induction of neuronal hyperexcitability (Robel S et al., 2015). Therefore, the significance of these findings is that it may provide a mechanism to explain both the cause of *GRIN2A*-associated epilepsies, as well as the fact that they often occur in adolescence and can sometimes resolve by adulthood (Gao K, et al., 2017; Li X et al., 2020).

Methodological Considerations and Alternative Explanations

The present histological data suggest that there is little difference in the baseline level of neuroinflammation between *Grin2a* KO and WT mice. The methodological rationale for staining microglia and astrocytes together via IBA1 and GFAP was to provide a general overview of the neuroinflammatory environment without the risk of getting lost in a single pathway (Kang JB et al., 2019; Norden DM et al., 2016). Given the well-established role of these two cell types in neuroinflammation caused by a wide variety of conditions (Franklin H et al., 2020), a macro-level view of the inflammatory

environment of the brain could be observed by measuring the area of these cells. Though GFAP and IBA1 immunostaining are common ways to detect these cell types, they too have limitations. GFAP is mainly expressed only in reactive astrocytes and is only noticeably expressed in primary processes in hippocampal astrocytes (Kamphuis W et al., 2012). Thus, there are entire astrocytes and large astrocyte regions that will not stain positive for GFAP. This is notable, since GluN2A-mediated changes to astrocyte number may only affect a certain sub-population of astrocytes or create changes to thin processes while leaving primary processes intact. If it so happens that the affected astrocytes or astrocyte areas are those that do not stain positive to GFAP, then current methods will fail to detect a greater change in astrocyte number and/or size that is truly present. Notably, undetectable thin processes are the components of the astrocyte that interact with synapses. This is important given that the effect of astrocytes on neuronal firing occurs in large part due to astrocytic regulation of neuronal synapses (Papouin T et al., 2017). However, it should also be noted that astrocytes in the mouse hippocampus do appear to stain for GFAP particularly well (Zhang Z et al., 2019).

For IBA1 staining of microglia, the greatest drawback is the question of selectivity. IBA1 is expressed in microglia under normal conditions. If there is an infiltration of peripheral monocytes into the brain, however, this will no longer be the case as these cells also stain positive for IBA1 (Gonzalez Ibanez F et al., 2019). Therefore, IBA1 is a reliable marker for microglia so long as the blood-brain barrier is intact, a condition which may not be true with *Grin2a* KO mice. It must be noted that there currently exists no evidence for this, however. Fortunately, IBA1 stains the entire cell and can even be used for morphological analysis (Tremblay ME et al., 2010) and

thus this stain does not share the same area/cell type limitations as GFAP. When assessing the data, these limitations of GFAP and IBA1 staining must be considered.

The present methods used assumed that changes in baseline neuroinflammation would be observable by changes in the area of GFAP and IBA1 expressing cells in the CA1 radiatum of mice. Therein lies another limitation of this method: regions other than the CA1 radiatum may be affected by the knockout. Additionally, the effects of knockout on neuroinflammation may be downstream from microglia and astrocytes. These two cell types are simply part of a larger neuroinflammatory cascade. There is evidence for the existence of NMDA receptors on peripheral immune cells, though the subunit composition is unknown (Boldyrev AA et al., 2012). Perhaps microglia and astrocytes are unaffected by the knockout under normal conditions, but the peripheral monocytes they recruit into the brain after an insult are modified in some way so as to provoke a runaway neuroinflammatory reaction. Another explanation is the possibility that at baseline, microglia and astrocytes undergo no change as a result of the Grin2a knockout. However, under very specific conditions of a particular insult, loss of the GluN2A subunit leads to a change in how these cell types react and ultimately the course of neuroinflammation in the brain.

Beyond the question of proteins and staining, the method of imaging is also an important factor to consider. The present data consist mostly of 3μm stacks of the brain slices. When single image analysis was performed, the variability of the data was extremely high. This would be expected, given that a z-stack effectively increases the number of technical replicates that compose each data point. Thus, variability due to random error would be expected to be lower and therefore the area of fluorescence

would approach their true values. The variability of the data may thus be lower if z-stacks were taken that encompass the entire slice. If there is a small difference at baseline, it may be masked in the variability of the imaging method.

Caution must be taken when attempting to translate the results of this experiment to that of human *GRIN2A* patients. *Grin2a* KO mice express no GluN2A protein, unlike most human patients who instead express a protein with lower glutamate/glycine potency. Truncation mutations are rare in humans, though there are some documented cases (see Supplementary Table S1).

Future Directions

The idea that changes in neuroinflammation in these models are downstream of microglia and astrocytes is supported by some preliminary evidence and should be explored further. Notably, in a pilot experiment performed in our lab, *Grin2a* KO mice had a greatly diminished peripheral immune response to lipopolysaccharide (LPS) injections compared to WT controls. Interestingly, however, stains of GFAP and IBA1 showed no discernable difference in fluorescence area between the two genotype conditions. This is quite remarkable when compared to the previously mentioned study wherein *Grin2a* knockout attenuated the neuroinflammatory response to LPS. Notably, in the aforementioned Grin2a KO LPS study (Francija E et al., 2019), neuroinflammation was measured by performing a Western Blot of IL-6, a pro-inflammatory cytokine. If it is indeed the case that there is no difference in IL-6 between genotypes after LPS, and that there is no difference in IBA1 and GFAP staining in genotypes mice after LPS, then it logically follows that the changes in neuroinflammation must be apparent via a

mechanism other than astrocyte expression of GFAP and microglial expression of IBA1. One potential mechanism is the production of reactive oxygen species, and the role that they have in redox regulation. Synaptic GluN2A is associated with the transcription of various redox regulating systems, such as the glutathione system (Baxter PS et al., 2015). This fact provides a next step in the path to test the theory of inflammatory instability; it may indeed be that the generation of reactive oxygen species (ROS), which is mostly downstream from the activation of microglia and astrocytes (given that these cells are the source of ROSs) in the cascade of neuroinflammation, is altered either at baseline or after insult with LPS (Sheng WS et al., 2013). Future work should therefore analyze the consequences of the activation of glial cells, such as generation of cytokines or ROSs, erosion of the blood-brain barrier, infiltration of peripheral immune cells, or epileptogenesis caused by neuroinflammation.

Other methods could also be used to account for the possibility that there are changes in baseline neuroinflammation that are not shown by immunohistochemistry. Alternatively, quantitative RT-PCR is a quick way to determine the relative expression of genes. However, success with this method depends on selecting genes of interest and brain regions to investigate. Changes in the mouse model may not lead to changes in levels of all cytokines or lead to neuroinflammation in all brain regions. Thus, which RNA to probe for must be carefully selected. Additionally, as the number of cytokines probed increases, the family-wise error rate must be accounted for. Future work could look at the expression of multiple pro- and anti-inflammatory cytokines such as interleukin-1β, interleukin-6, tumor necrosis factor-α, C-C motif ligand 2, C-X-C motif chemokine ligand 10, interleukin-10, and interleukin-4. Additionally, Western Blots can

be used to detect the expression of proteins that are involved in redox regulation in the brain, such as glutathione, or a different part of the neuroinflammatory cascade such as mitogen-activated protein kinase (MAPK). This pathway is activated in response to nearly all cytokines and is well-understood in the context of inflammation (Kaminska B et al., 2009). Finally, other qualities of microglia and astrocytes could be analyzed. For example, proliferation of these cell types can be measured. Bromodeoxyuridine (BrdU) can be administered to animals where it is preferentially taken up by rapidly dividing cells and then visualized using anti-BrdU antibodies. By colocalizing this stain with either GFAP or IBA1, rapidly dividing astrocytes or microglia can be detected, respectively (Susarla BT et al., 2014). Another example is colocalizing these stains with Ki-67, a cellular marker for proliferating cells (Scholzen T and Gerdes J, 2000). Finally, counting cell bodies or morphology can give another measure of these glial cells. This is possible with IBA1 for microglia, however a different stain would need to be used in astrocytes to ensure staining of thin processes. One such stain for astrocytes is aldehyde dehydrogenase 1 family member L1 (AldhL1) (Preston AN et al., 2019).

The interesting mix of previous work that suggests both a general resistance to neuroinflammation combined with instances of unregulated inflammation suggest that *Grin2a* KO mice contain some sort of pathway-dependent neuroinflammatory susceptibility. The main focus of future work should be to better characterize the conditions of this susceptibility. The unpublished data using LPS and heat to induce febrile seizures, as well as the ability of a dopamine reuptake inhibitor to induce lasting redox dysregulation, strongly suggest that this mouse model contains a difference in neuroinflammation compared to WT controls. However, other research suggesting

610 resistance to neuroinflammation when administered LPS makes it clear that any
611 difference in neuroinflammation is likely pathway-dependent. Though this present
612 research attempted to look at more general markers of neuroinflammation, the
613 subtleties of the *Grin2a* knockout mouse model may demand a closer look at a specific
614 aspect of neuroinflammation, or at neuroinflammation after a specific insult.
615
616
617
618
619
620
621
622
623
624
625
626
627
628
629
630
631
632

References

Abbott NJ, Ronnback L, Hansson E (2006), Astrocyte-endothelial interactions at the blood-brain barrier. Nat Rev Neurosci 7:41-53.

Al Sufiani F, Ang LC (2012), Neuropathology of temporal lobe epilepsy. Epilepsy Res Treat 2012:624519.

Andoh M, Ikegaya Y, Koyama R (2019), Synaptic Pruning by Microglia in Epilepsy. J Clin Med 8.

Babb TL, Wilson CL, Isokawa-Akesson M (1987), Firing patterns of human limbic neurons during stereoencephalography (SEEG) and clinical temporal lobe seizures. Electroencephalogr Clin Neurophysiol 66:467-482.

Bar-Shira O, Maor R, Chechik G (2015), Gene Expression Switching of Receptor Subunits in Human Brain Development. PLoS Comput Biol 11:e1004559.

Barnes PJ (2006), How corticosteroids control inflammation: Quintiles Prize Lecture 2005. Br J Pharmacol 148:245-254.

Baxter PS, Bell KF, Hasel P, Kaindl AM, Fricker M, Thomson D, Cregan SP, Gillingwater TH, et al. (2015), Synaptic NMDA receptor activity is coupled to the transcriptional control of the glutathione system. Nat Commun 6:6761.

Billiau AD, Witters P, Ceulemans B, Kasran A, Wouters C, Lagae L (2007), Intravenous immunoglobulins in refractory childhood-onset epilepsy: effects on seizure frequency, EEG activity, and cerebrospinal fluid cytokine profile. Epilepsia 48:1739-1749.

Blumenfeld H (2012), Impaired consciousness in epilepsy. Lancet Neurol 11:814-826.

Boldyrev AA, Bryushkova EA, Vladychenskaya EA (2012), NMDA receptors in immune competent cells. Biochemistry (Mosc) 77:128-134.

Cardis R, Cabungcal JH, Dwir D, Do KQ, Steullet P (2018), A lack of GluN2A-containing NMDA receptors confers a vulnerability to redox dysregulation: Consequences on parvalbumin interneurons, and their perineuronal nets. Neurobiol Dis 109:64-75.

Carvill GL, Regan BM, Yendle SC, O'Roak BJ, Lozovaya N, Bruneau N, Burnashev N, Khan A, et al. (2013), GRIN2A mutations cause epilepsy-aphasia spectrum disorders. Nat Genet 45:1073-1076.

662 Chang KH, Hsu YC, Chang MY, Lin CL, Wu TN, Hwang BF, Chen CY, Liu HC, et al. (2015),
663 A Large-Scale Study Indicates Increase in the Risk of Epilepsy in Patients With Different Risk
664 Factors, Including Rheumatoid Arthritis. Medicine (Baltimore) 94:e1485.

665 Cotman C, Monaghan D (1989), Multiple excitatory amino acid receptor regulation of
666 intracellular Ca2+. Implications for aging and Alzheimer's disease. Ann N Y Acad Sci 568:138-
667 148.

668 Das A, Wallace GCt, Holmes C, McDowell ML, Smith JA, Marshall JD, Bonilha L, Edwards
669 JC, et al. (2012), Hippocampal tissue of patients with refractory temporal lobe epilepsy is
670 associated with astrocyte activation, inflammation, and altered expression of channels and
671 receptors. Neuroscience 220:237-246.

672 de Lanerolle NC, Lee TS, Spencer DD (2010), Astrocytes and epilepsy. Neurotherapeutics
673 7:424-438.

674 Dey A, Kang X, Qiu J, Du Y, Jiang J (2016), Anti-Inflammatory Small Molecules To Treat
675 Seizures and Epilepsy: From Bench to Bedside. Trends Pharmacol Sci 37:463-484.

676 Duncan JS, Sander JW, Sisodiya SM, Walker MC (2006), Adult epilepsy. Lancet 367:1087-
677 1100.

678 Eng LF, Ghirnikar RS, Lee YL (2000), Glial fibrillary acidic protein: GFAP-thirty-one years
679 (1969-2000). Neurochem Res 25:1439-1451.

680 Eyo UB, Bispo A, Liu J, Sabu S, Wu R, DiBona VL, Zheng J, Murugan M, et al. (2018), The
681 GluN2A Subunit Regulates Neuronal NMDA receptor-Induced Microglia-Neuron Physical
682 Interactions. Sci Rep 8:828.

683 Fisher RS, Acevedo C, Arzimanoglou A, Bogacz A, Cross JH, Elger CE, Engel J, Jr., Forsgren
684 L, et al. (2014), ILAE official report: a practical clinical definition of epilepsy. Epilepsia 55:475-
685 482.

686 Francija E, Petrovic Z, Brkic Z, Mitic M, Radulovic J, Adzic M (2019), Disruption of the
687 NMDA receptor GluN2A subunit abolishes inflammation-induced depression. Behav Brain Res
688 359:550-559.

689 Franklin H, Clarke BE, Patani R (2020), Astrocytes and microglia in neurodegenerative diseases:
690 Lessons from human in vitro models. Prog Neurobiol:101973.

691 Gao K, Tankovic A, Zhang Y, Kusumoto H, Zhang J, Chen W, XiangWei W, Shaulsky GH, et
692 al. (2017), A de novo loss-of-function GRIN2A mutation associated with childhood focal
693 epilepsy and acquired epileptic aphasia. PLoS One 12:e0170818.

694 Ge M, Song H, Li H, Li R, Tao X, Zhan X, Yu N, Sun N, et al. (2019), Memory Susceptibility to
695 Retroactive Interference Is Developmentally Regulated by NMDA Receptors. Cell Rep 26:2052-
696 2063 e2054.

697 Gonzalez Ibanez F, Picard K, Bordeleau M, Sharma K, Bisht K, Tremblay ME (2019),
698 Immunofluorescence Staining Using IBA1 and TMEM119 for Microglial Density, Morphology
699 and Peripheral Myeloid Cell Infiltration Analysis in Mouse Brain. J Vis Exp.

700 Hansen KB, Yi F, Perszyk RE, Menniti FS, Traynelis SF (2017), NMDA Receptors in the
701 Central Nervous System. Methods Mol Biol 1677:1-80.

702 Harris KM, Weinberg RJ (2012), Ultrastructure of synapses in the mammalian brain. Cold
703 Spring Harb Perspect Biol 4.

704 Harry GJ, Kraft AD (2008), Neuroinflammation and microglia: considerations and approaches
705 for neurotoxicity assessment. Expert Opin Drug Metab Toxicol 4:1265-1277.

706 Hausman-Kedem M, Menascu S, Greenstein Y, Fattal-Valevski A (2020), Immunotherapy for
707 GRIN2A and GRIN2D-related epileptic encephalopathy. Epilepsy Res 163:106325.

708 Henley JM, Wilkinson KA (2016), Synaptic AMPA receptor composition in development,
709 plasticity and disease. Nat Rev Neurosci 17:337-350.

710 Hiragi T, Ikegaya Y, Koyama R (2018), Microglia after Seizures and in Epilepsy. Cells 7.

711 Hizue M, Pang CH, Yokoyama M (2005), Involvement of N-methyl-D-aspartate-type glutamate
712 receptor epsilon1 and epsilon4 subunits in tonic inflammatory pain and neuropathic pain.
713 Neuroreport 16:1667-1670.

714 Holtman IR, Raj DD, Miller JA, Schaafsma W, Yin Z, Brouwer N, Wes PD, Moller T, et al.
715 (2015), Induction of a common microglia gene expression signature by aging and
716 neurodegenerative conditions: a co-expression meta-analysis. Acta Neuropathol Commun 3:31.

717 Kaminska B, Gozdz A, Zawadzka M, Ellert-Miklaszewska A, Lipko M (2009), MAPK signal
718 transduction underlying brain inflammation and gliosis as therapeutic target. Anat Rec
719 (Hoboken) 292:1902-1913.

720 Kamphuis W, Mamber C, Moeton M, Kooijman L, Sluijs JA, Jansen AH, Verveer M, de Groot
721 LR, et al. (2012), GFAP isoforms in adult mouse brain with a focus on neurogenic astrocytes and
722 reactive astrogliosis in mouse models of Alzheimer disease. PLoS One 7:e42823.

723 Kang JB, Park DJ, Shah MA, Kim MO, Koh PO (2019), Lipopolysaccharide induces neuroglia
724 activation and NF-kappaB activation in cerebral cortex of adult mice. Lab Anim Res 35:19.

725 Kapur (2018), Role of NMDA Receptors in the pathophysiology and treatment of status
726 epilepticus. Epilepsia Open 3:165-168.

727 Keaney J, Campbell M (2015), The dynamic blood-brain barrier. FEBS J 282:4067-4079.

728 Kew JN, Kemp JA (2005), Ionotropic and metabotropic glutamate receptor structure and
729 pharmacology. Psychopharmacology (Berl) 179:4-29.

730 Kwon HS, Koh SH (2020), Neuroinflammation in neurodegenerative disorders: the roles of
731 microglia and astrocytes. Transl Neurodegener 9:42.

732 Lerma J (2003), Roles and rules of kainate receptors in synaptic transmission. Nat Rev Neurosci
733 4:481-495.

734 Li X, Xie LL, Han W, Hong SQ, Ma JN, Wang J, Jiang L (2020), Clinical Forms and GRIN2A
735 Genotype of Severe End of Epileptic-Aphasia Spectrum Disorder. Front Pediatr 8:574803.

736 Li Z, Martins da Silva A, Cunha JP (2002), Movement quantification in epileptic seizures: a new
737 approach to video-EEG analysis. IEEE Trans Biomed Eng 49:565-573.

738 Liu XB, Murray KD, Jones EG (2004), Switching of NMDA receptor 2A and 2B subunits at
739 thalamic and cortical synapses during early postnatal development. J Neurosci 24:8885-8895.

740 Loewen JL, Barker-Haliski ML, Dahle EJ, White HS, Wilcox KS (2016), Neuronal Injury,
741 Gliosis, and Glial Proliferation in Two Models of Temporal Lobe Epilepsy. J Neuropathol Exp
742 Neurol 75:366-378.

743 Lu J, Huang H, Zeng Q, Zhang X, Xu M, Cai Y, Wang Q, Huang Y, et al. (2019), Hippocampal
744 neuron loss and astrogliosis in medial temporal lobe epileptic patients with mental disorders. J
745 Integr Neurosci 18:127-132.

746 Luscher C, Malenka RC (2012), NMDA receptor-dependent long-term potentiation and long-
747 term depression (LTP/LTD). Cold Spring Harb Perspect Biol 4.

748 Mamber C, Kamphuis W, Haring NL, Peprah N, Middeldorp J, Hol EM (2012), GFAPdelta
749 expression in glia of the developmental and adolescent mouse brain. PLoS One 7:e52659.

750 Masia SL, Devinsky O (2000), Epilepsy and behavior: a brief history. Epilepsy Behav 1:27-36.

751 Matejuk A, Ransohoff RM (2020), Crosstalk Between Astrocytes and Microglia: An Overview.
752 Front Immunol 11:1416.

753 McKay S, Ryan TJ, McQueen J, Indersmitten T, Marwick KFM, Hasel P, Kopanitsa MV, Baxter
754 PS, et al. (2018), The Developmental Shift of NMDA Receptor Composition Proceeds
755 Independently of GluN2 Subunit-Specific GluN2 C-Terminal Sequences. Cell Rep 25:841-851
756 e844.

757 McLeod F, Marzo A, Podpolny M, Galli S, Salinas P (2017), Evaluation of Synapse Density in
758 Hippocampal Rodent Brain Slices. J Vis Exp.

759 Myers KA, Scheffer IE (1993) GRIN2A-Related Speech Disorders and Epilepsy. In:
760 GeneReviews((R)), vol. (Adam MP, Ardinger HH, Pagon RA, Wallace SE, Bean LJH, Mirzaa
761 G, Amemiya A, eds). Seattle (WA).

762 Norden DM, Trojanowski PJ, Villanueva E, Navarro E, Godbout JP (2016), Sequential
763 activation of microglia and astrocyte cytokine expression precedes increased Iba-1 or GFAP
764 immunoreactivity following systemic immune challenge. Glia 64:300-316.

765 Ohsawa K, Imai Y, Kanazawa H, Sasaki Y, Kohsaka S (2000), Involvement of Iba1 in
766 membrane ruffling and phagocytosis of macrophages/microglia. J Cell Sci 113 (Pt 17):3073-
767 3084.

768 Paoletti P, Bellone C, Zhou Q (2013), NMDA receptor subunit diversity: impact on receptor
769 properties, synaptic plasticity and disease. Nat Rev Neurosci 14:383-400.

770 Papouin T, Dunphy J, Tolman M, Foley JC, Haydon PG (2017), Astrocytic control of synaptic
771 function. Philos Trans R Soc Lond B Biol Sci 372.

772 Pekny M, Pekna M (2016), Reactive gliosis in the pathogenesis of CNS diseases. Biochim
773 Biophys Acta 1862:483-491.

774 Perry VH, Nicoll JA, Holmes C (2010), Microglia in neurodegenerative disease. Nat Rev Neurol
775 6:193-201.

776 Petralia RS, Wang YX, Wenthold RJ (1994), The NMDA receptor subunits NR2A and NR2B
777 show histological and ultrastructural localization patterns similar to those of NR1. J Neurosci
778 14:6102-6120.

779 Platt SR (2007), The role of glutamate in central nervous system health and disease--a review.
780 Vet J 173:278-286.

781 Preston AN, Cervasio DA, Laughlin ST (2019), Visualizing the brain's astrocytes. Methods
782 Enzymol 622:129-151.

783 Raghunatha P, Vosoughi A, Kauppinen TM, Jackson MF (2020), Microglial NMDA receptors
784 drive pro-inflammatory responses via PARP-1/TRMP2 signaling. Glia 68:1421-1434.

785 Rana A, Musto AE (2018), The role of inflammation in the development of epilepsy. J
786 Neuroinflammation 15:144.

787 Robel S, Buckingham SC, Boni JL, Campbell SL, Danbolt NC, Riedemann T, Sutor B,
788 Sontheimer H (2015), Reactive astrogliosis causes the development of spontaneous seizures. J
789 Neurosci 35:3330-3345.

790 Sakimura K, Kutsuwada T, Ito I, Manabe T, Takayama C, Kushiya E, Yagi T, Aizawa S, et al.
791 (1995), Reduced hippocampal LTP and spatial learning in mice lacking NMDA receptor epsilon
792 1 subunit. Nature 373:151-155.

793 Scholzen T, Gerdes J (2000), The Ki-67 protein: from the known and the unknown. J Cell
794 Physiol 182:311-322.

795 Sheng WS, Hu S, Feng A, Rock RB (2013), Reactive oxygen species from human astrocytes
796 induced functional impairment and oxidative damage. Neurochem Res 38:2148-2159.

797 Skowronska K, Obara-Michlewska M, Zielinska M, Albrecht J (2019), NMDA Receptors in
798 Astrocytes: In Search for Roles in Neurotransmission and Astrocytic Homeostasis. Int J Mol Sci
799 20.

800 Sofroniew MV, Vinters HV (2010), Astrocytes: biology and pathology. Acta Neuropathol 119:7-
801 35.

802 Stichel CC, Muller HW (1998), The CNS lesion scar: new vistas on an old regeneration barrier.
803 Cell Tissue Res 294:1-9.

804 Susarla BT, Villapol S, Yi JH, Geller HM, Symes AJ (2014), Temporal patterns of cortical
805 proliferation of glial cell populations after traumatic brain injury in mice. ASN Neuro 6:159-170.

806 Tremblay ME, Lowery RL, Majewska AK (2010), Microglial interactions with synapses are
807 modulated by visual experience. PLoS Biol 8:e1000527.

808 Trinka E, Cock H, Hesdorffer D, Rossetti AO, Scheffer IE, Shinnar S, Shorvon S, Lowenstein
809 DH (2015), A definition and classification of status epilepticus--Report of the ILAE Task Force
810 on Classification of Status Epilepticus. Epilepsia 56:1515-1523.

811 van Rossum D, Hanisch UK (2004), Microglia. Metab Brain Dis 19:393-411.

812 Vezzani A, Dingledine R, Rossetti AO (2015), Immunity and inflammation in status epilepticus
813 and its sequelae: possibilities for therapeutic application. Expert Rev Neurother 15:1081-1092.

814 Wyllie DJ, Livesey MR, Hardingham GE (2013), Influence of GluN2 subunit identity on NMDA
815 receptor function. Neuropharmacology 74:4-17.

816 XiangWei W, Jiang Y, Yuan, H (2017), *De Novo* Mutations and Rare Variants Occuring in
817 NMDA receptors. Curr Opin Physiol 2:27-35

818 Xin WK, Kwan CL, Zhao XH, Xu J, Ellen RP, McCulloch CA, Yu XM (2005), A functional
819 interaction of sodium and calcium in the regulation of NMDA receptor activity by remote
820 NMDA receptors. J Neurosci 25:139-148.

821 Yuan H, Low CM, Moody OA, Jenkins A, Traynelis SF (2015), Ionotropic GABA and
822 Glutamate Receptor Mutations and Human Neurological Diseases. Molecular Pharmacology
823 99:97998

824 Zhang Z, Ma Z, Zou W, Guo H, Liu M, Ma Y, Zhang L (2019), The Appropriate Marker for
825 Astrocytes: Comparing the Distribution and Expression of Three Astrocytic Markers in Different
826 Mouse Cerebral Regions. Biomed Res Int 2019:9605265.

827 Zhu S, Stein RA, Yoshioka C, Lee CH, Goehring A, McHaourab HS, Gouaux E (2016),
828 Mechanism of NMDA Receptor Inhibition and Activation. Cell 165:704-714.
829

830

831

832

833

834

835

836

837

838

839

840 **Supplementary Table S1**

Gene	Protein Change	Domain	cDNA change	RefSeq	gnomAD Alleles	Class	Phenotype
GRIN2A	p. Tyr 1387*	CTD					CSWSS (proband
GRIN2A	p.Ala243Val	ATD	c.728C>T	NM_000833.4	0	unk	RE; ID
GRIN2A	p.Pro552Arg	S1-M1	c.1655C>G	NM_000833.3	0	DM	EPI; ID; no speech
GRIN2A	p.Ala635Thr	M3	c.1903G>A	NM_000833.4	0		
GRIN2A	p.Val639Ile	M3	c.1915G>A	NM_000833.4	0		
GRIN2A	p.Leu642Met	M3	c.1924C>A	NM_000833.4	0		
GRIN2A	p.Ala643Asp	M3	c.1928C>A	NM_000833.3	0	DM (germinal mosaicism)	DD; ID; Dystonia;
GRIN2A	p.Ser644Gly	M3	c.1930A>G	NM_000833.3	0		
GRIN2A	p.Thr646Ala	M3	c.1936A>G	NM_000833.4	0	DM	EE
GRIN2A	p.Leu649Val	M3	c.1945C>G	NM_000833.4	0	DM	ID; EPI; feeding ir dysmorphism
GRIN2A	p.Phe652Val	M3	c.1954T>G	NM_000833.4	0	DM	CSWSS; ASD
GRIN2A	p.Ile654Thr	M3	c.1961T>C	NM_000833.4	0		
GRIN2A	p.Lys669Asn	S2	c.2007G>T	NM_000833.3	0	DM	RE; CSWSS
GRIN2A	p.Arg681Gln	S2	c.2042G>A	NM_000833.4	0		
GRIN2A	p.Arg695Gln	S2	c.2084G>A	NM_000833.4	0		
GRIN2A	p.Pro699Ser	S2	c.2095C>T	NM_000833.3	0	DM	BECTS
GRIN2A	p.Lys804Thr	S2-M4	c.2411A>C	NM_000833.4	0		
GRIN2A	p.Ser809Arg	S2-M4	c.2427C>A	NM_000833.4	0		
GRIN2A	p.Leu812Met	S2-M4	c.2434C>A	NM_000833.3	0	DM	Epileptic enceph

GRIN2A	p.Met817Val	M4	c.2449A>G	NM_000833.3	0	DM	DD; EPI; ID
GRIN2A	p.Ala818Glu	M4	c.2453C>A	NM_000833.4	0		
GRIN2A	p.Lys1005Arg	CTD	c.3014A>G	NM_000833.3	0		
GRIN2A	p.Tyr676Asn	S2	c.2026T>A	NM_000833.4	1		
GRIN2A	p.Pro678Leu	S2	c.2033C>T	NM_000833.4	1		
GRIN2A	p.Gly744Val	S2	c.2231G>T	NM_000833.4	1		
GRIN2A	p.Gly768Asp	S2	c.2303G>A	NM_000833.4	1		
GRIN2A	p.Ala818Val	M4	c.2453C>T	NM_000833.4	1		
GRIN2A	p.Ala827Thr	M4	c.2479G>A	NM_000833.4	1		
GRIN2A	p.Arg1402Pro	CTD	c.4205G>C	NM_000833.4	1		
GRIN2A		-	dup chr16: 10 075 000–10 225 000 (hg19)	Het			
GRIN2A	p.Val452Met	S2	c.1354G>A			DM	SCZ; intractable s
GRIN2A	p.Ala1276Gly (3)	CTD	c.3827C>G				CSWSS (2); BECTS
GRIN2A	p.Gln655Lys	M3-S2	0				-
GRIN2A	p.Met1Thr	ATD	c.2T>C	NM_000833.3	0	trans; unk	LKS; LD; seizures-
GRIN2A	p.Pro31Thr	ATD	c.91C>A	NM_000833.3	0		EPI
GRIN2A	p.Phe183Ile	ATD	c.547T>A	NM_000833.4	0	trans	BECTS; DD (fathe
GRIN2A	p.Ile184Ser	ATD	c.551T>G	NM_000833.4	0	DM; trans	CSWSS (mother u
GRIN2A	p.His223Tyr	ATD	c.667C>T	NM_000833.4	0		
GRIN2A	p.Cys231Arg	ATD	c.691T>C	NM_000833.4	0		
GRIN2A	p.Cys231Tyr	ATD	c.692G>A	NM_000833.4	0	trans	LKS; CTS; ID (mot
GRIN2A	p.Gly247Ser	ATD	c.739G>A	NM_000833.4	0		

GRIN2A	p.Leu411Gln	S1	c.1232T>A	NM_000833.4	0		
GRIN2A	p.Cys436Arg	S1	c.1306T>C	NM_000833.3	0	DM	ABPE
GRIN2A	p.Glu448Lys	S1	c.1342G>A	NM_000833.4	0		
GRIN2A	p.Ile461Asn	S1	c.1382T>A	NM_000833.4	0		
GRIN2A	p.Gly483Arg	S1	c.1447G>A	NM_000833.3	0	trans; unk	CSWSS+dysphasi
GRIN2A	p.Gly498Ser	S1	c.1492G>A	NM_000833.4	0		
GRIN2A	p.Val500Gly	S1	c.1499T>G	NM_000833.4	0		
GRIN2A	p.Val506Ala	S1	c.1517T>C	NM_000833.3	0	trans	focal seizures
GRIN2A	p.Arg518His	S1	c.1553G>A	NM_000833.3	0	trans; unk	CSWSS; RE; verba
GRIN2A	p.Pro527Arg	S1	c.1580C>G	NM_000833.4	0		
GRIN2A	p.Val529Trpfs X22	S1	c.1585delG	NM_000833.3	0	trans	ID; RE; MD; LD
GRIN2A	p.Thr531Met	S1	c.1592C>T	NM_000833.4	0	trans; unk	EPI (aphasia); LD;
GRIN2A	p.Ser545Leu	S1-M1	c.1634C>T	NM_000833.3	0	trans	LD
GRIN2A	p.Ala548Thr	S1-M1	c.1642G>A	NM_000833.3	0	DM	LKS
GRIN2A	p.Ser556Ala	M1	c.1666T>G	NM_000833.4	0		
GRIN2A	p.Ser556Phe	M1	c.1667C>T	NM_000833.4	0		
GRIN2A	p.Thr684Ala	S2	c.2050A>G	NM_000833.4	0		
GRIN2A	p.Val685Gly	S2	c.2054T>G	NM_000833.3	0	DM	severe intractabl
GRIN2A	p.Ile694Thr	S2	c.2081T>C	NM_000833.3	0	DM	LKS; EPI
GRIN2A	p.Met705Val	S2	c.2113A>G	NM_000833.3	0	trans	BECTS (mother, s

GRIN2A	p.Val713Gly	S2	c.2138T>G	NM_000833.4	0		
GRIN2A	p.Glu714Lys	S2	c.2140G>A	NM_000833.3	0	unk	CSWSS
GRIN2A	p.Ala727Thr	S2	c.2179G>A	NM_000833.3	0	unk	RE; BECTS
GRIN2A	p.Asp731Asn	S2	c.2191G>A	NM_000833.3	0	trans; DM	RE; verbal dyspra
GRIN2A	p.Ala733Thr	S2	c.2197G>A	NM_000833.4	0		
GRIN2A	p.Val734Leu	S2	c.2200G>C	NM_000833.3	0	trans	BECTS (mother u
GRIN2A	p.Gly760Val	S2	c.2279G>T	NM_000833.3	0		
GRIN2A	p.Lys772Glu	S2	c.2314A>G	NM_000833.3	0	unk	ABPE; ID; reading
GRIN2A	p.Asp776Tyr	S2	c.2326G>T	NM_000833.4	0		
GRIN2A	p.Glu803Lys	S2-M4	c.2407G>A	NM_000833.4	0		
GRIN2A	p.Ile876Ala	CTD	c.2626-7AT>GC	NM_000833.3	0		
GRIN2A	p.Tyr943Ter	CTD	c.2829C>G	NM_000833.3	0	trans	CSWS
GRIN2A	p.Asn1274Ser	CTD	c.3821A>G	NM_000833.4	0		
GRIN2A	p.Pro79Arg	ATD	c.236C>G	NM_000833.4	1	trans	CSWSS; RE; ADHD unaffected)
GRIN2A	p.Arg370Trp	ATD	c.1108C>T	NM_000833.3	1	unk	BECTS
GRIN2A	p.Lys457Glu	S1	c.1369A>G	NM_000833.4	1		
GRIN2A	p.Arg504Trp	S1	c.1510C>T	NM_000833.3	1	trans	DD; CSWSS; FS
GRIN2A	p.Arg518Cys	S1	c.1552C>T	NM_000833.3	1	trans	CSWSS; RE; dyspr
GRIN2A	p.Phe682Ser	S2	c.2045T>C	NM_000833.4	1		

GRIN2A	p.Thr690Met	S2	c.2069C>T	NM_00083 3.3	1	DM	EPI
GRIN2A	p.Met701Val	S2	c.2101A>G	NM_00083 3.4	1		
GRIN2A	p.Ala716Thr	S2	c.2146G>A	NM_00083 3.4	1	trans; DM	RE; ID; verbal dys
GRIN2A	p.Glu743Asp	S2	c.2229A>C	NM_00083 3.4	1		
GRIN2A	p.Ile775Met	S2	c.2325C>G	NM_00083 3.4	1		
GRIN2A	p.Asp776Asn	S2	c.2326G>A	NM_00083 3.4	1		
GRIN2A	p.Gly784Ala	S2	c.2351G>C	NM_00083 3.4	1		
GRIN2A	p.Gln811Pro	S2-M4	c.2432A>C	NM_00083 3.4	1		
GRIN2A	p.Met828Thr	M4	c.2483T>C	NM_00083 3.4	1		
GRIN2A	p.Pro857Ala	CTD	c.2569C>G	NM_00083 3.4	1		
GRIN2A	p.Asp615Lys	M2					Infantile spasms;
GRIN2A	p.Val734Leu	S2				trans	RE
GRIN2A	p.Trp198*	ATD					ABPE
GRIN2A	p.Gln218*	ATD				trans	Moderate ID + CT learning difficulti learning difficulti
GRIN2A	p.Leu334*	ATD				trans	CSWSS (proband (brother), partial
GRIN2A	p.Tyr943*	CTD				trans	CSWSS (proband
GRIN2A		-	del chr16: 9 850 000–9 900 000 (hg19)				ABPE
GRIN2A		-	del chr16: 9 825 000–10 075 000 (hg19)				
GRIN2A		-	del chr16: 10 250 000–10 275 000 (hg19)				RE
GRIN2A		-	del chr16: 7 964 000–10 607 500 (hg19)				Pseudo-Lennox S
GRIN2A	p.Lys592fs (predicted)	M2	del chr16: 8 992 500–9 992 500 (hg19)				RE + Moderate ID

GRIN2A		-	del chr16: 9 365 500–11 273 700 (hg19)				Myoclonic seizur
GRIN2A		CTD	del chr16: 9 809 522–9 856 618 (hg19)				RE + Mild ID
GRIN2A		S2	del chr16: 9 908 477–9 934 830 (hg19) (2)			trans	LKS (proband); LK
GRIN2A		-	del chr16: 10 227 121–10 354 862 (hg19)			trans	CSWSS + VD (thre
GRIN2A		-	16p13.2 microdeletion			trans	Focal seizures + D unaffected)
GRIN2A		-	16p13.2p13.13 microduplication			*DM*	Epilepsy + ID + De
GRIN2A	p.Arg504Trp	S1	c.1510C>T			trans	CSWSS (proband,
GRIN2A	p.Ala716Thr	S2	c.2146G>A			trans	RE + Verbal dyspr dyxprax (cousin); coordination
GRIN2A	p.Ile904Phe	CTD	c.2710A>T	NM_000833.4	0	trans	RE; Febrile seizur
GRIN2A	p.Asp933Asn	CTD	c.2797G>A	NM_000833.4	0	trans	LKS
GRIN2A	p.Ile814Thr	S2-M4	c. 2441T>C				RE; benign epilep
GRIN2A	p.Asn976Ser	CTD	c.2927A>G				ABPE; CSWS
GRIN2A	p.Arg586Lys	M1-M2	c.1757G>A			trans	Severe EE (paren ID
GRIN2A	°IVS7	S2	c.2007+1G>A			DM; trans (father not affected)	CSWSS; LD
GRIN2A	p.Phe528Glyfs*22	S1	c.1586delT het.			likely trans	Continuous Spike severe LD
GRIN2A	p.Trp606*	M2	c.1818G>A het.			unknown	ABPE; LD
GRIN2A	p.Glu803*	S2-M4	c.2407G>T het.			DM	LKS
GRIN2A	n.a	-	duplication exon 4 & 5 het.			unknown	Epileptic encepha
GRIN2A	p.?	S1-M1	c.1652-1G > A			DM	EAS
GRIN2A	p. Gly668Ala	S2	c.G2063>C			DM	specific language

GRIN2A	p.Pro31SerfsX107	ATD	c.90delTins(T)2	NM_000833.3	0	trans	BECTS (mother a
GRIN2A	p.Trp55Ter	ATD	c.165G>A	NM_000833.4	0		
GRIN2A	p.Arg94Gly	ATD	c.280C>G	NM_000833.4	0		
GRIN2A	p.Ile95Thr	ATD	c.284C>T	NM_000833.4	0		
GRIN2A	p.Ala136Ser	ATD	c.406G>T	NM_000833.4	0		
GRIN2A	p.Lys138Thr	ATD	c.413>A>C	NM_000833.4	0		
GRIN2A	p.Thr143Ile	ATD	c.482C>T	NM_000833.3	0	DM	ASD
GRIN2A	p.Thr143Ile	ATD	c.482C>T	NM_000833.3	0		
GRIN2A	p.Leu159Pro	ATD	c.476T>C	NM_000833.3	0		
GRIN2A	p.Gln163Ter	ATD	c.487C>T	NM_000833.4	0		pathogenic (not s
GRIN2A	p.Thr189Asn	ATD	c.566C>A	NM_000833.4	0		ASD
GRIN2A	p.Trp198Ter	ATD	c.594G>A	NM_000833.3	0	unk	ABPE
GRIN2A	p.Leu206Pro	ATD	c.617T>C	NM_000833.4	0		
GRIN2A	p.Gln218Ter	ATD	c.652C>T	NM_000833.3	0	DM; trans	ID; EPI in infancy
GRIN2A	p.Ile313Thr	ATD	c.938T>C	NM_000833.4	0		
GRIN2A	p.Leu334Ter	ATD	c.1001T>A	NM_000833.3	0	trans	CSWS
GRIN2A		ATD	c.1007+1G>A; c.1007+1G>T	NM_000833.3	0	unk; trans	REy+verbal dyspr affected)
GRIN2A	p.Val339Phe	ATD	c.1015G>T	NM_000833.4	0		
GRIN2A	p.Val375fs	ATD	c.1123-2A>G	NM_000833.3	0	trans	EPI; LD; CSWSS; F
GRIN2A	p.Trp390Cys	ATD-S1	c.1170G>T	NM_000833.4	0		
GRIN2A	p.Leu425Val	S1	c.1273C>G	NM_000833.4	0		
GRIN2A	p.Phe439Leu	S1	c.1317C>G	NM_000833.4	0		

GRIN2A	p.Cys455Tyr	S1	c.1364G>A	NM_000833.3	0		
GRIN2A	p.Ser511Leu	S1	c.1532C>T	NM_000833.4	0		
GRIN2A	p.Arg518Leu	S1	c.1553G>T	NM_000833.3	0		
GRIN2A	p.Gly532Val	S1	c.1595G>T	NM_000833.4	0		
GRIN2A	p.Ser547del	S1-M1	c.1637_1639delTCT	NM_000833.3	0		ID; EPI; MD; LD;
GRIN2A	p.Ala548Pro	S1-M1	c.1642G>C	NM_000833.3	0		
GRIN2A	p.Glu551Lys	S1-M1	c.1651G>A	NM_000833.4	0		
GRIN2A	p.Ser554Thr	S1-M1	c.1661G>C	NM_000833.3	0		
GRIN2A	p.Trp558Ser	M1	c.1673G>C	NM_000833.4	0		
GRIN2A	p.Met561del	M1	c.1681-83delATG	NM_000833.4	0		
GRIN2A	p.Phe562LeufsX2	M1	?	NM_000833.4	0		
GRIN2A	p.Met564IlefsX8	M1	?	NM_000833.4	0		
GRIN2A	p.Phe576Ser	M1	c.1728T>A	NM_000833.4	0		
GRIN2A	p.Phe599Leu	M2		NM_000833.4	0		
GRIN2A	p.Leu611Gln	M2	c.1832T>A	NM_000833.4	0		
GRIN2A	p.Asn614Ser	M2	c.1841A>G	NM_000833.4	0	DM	focal epilepsy; LD
GRIN2A	p.Asn615Ser	M2	c.1844A>G	NM_000833.4	0		
GRIN2A	p.Asn615Lys	M2	c.1845C>A	NM_000833.4	0	DM	EPI; DD; EOEE(?);
GRIN2A	p.Ser632Phe	M3	c.1895C>T	NM_000833.4	0		
GRIN2A	p.Trp634Ter	M3	c.1901G>A	NM_000833.4	0		
GRIN2A	p.Ala638Val	M3	c.1913C>T	NM_000833.4	0		

GRIN2A	p.Thr646Arg	M3	c.1937C>G	NM_000833.4	0		
GRIN2A	p.Asn648Ser	M3	c.1943A>G	NM_000833.4	0		
GRIN2A	p.Asn649Pro	M3	c.1946_1947delinsCT	NM_000833.4	0		
GRIN2A	p.Met653Ile	M3	c.1959G>A	NM_000833.4	0		
GRIN2A	p.Met653Val	M3		NM_000833.3	0	DM	
GRIN2A	p.Gln661Ter	S2	c.1981C>T	NM_000833.4	0		
GRIN2A	p.Arg681Ter	S2	c.2041C>T	NM_000833.3	0	trans	LKS
GRIN2A	p.Met701Ile	S2	c.2103G>C	NM_000833.4	0		
GRIN2A	p.Ala702Thr	S2	cDNA change	NM_000833.4	0		
GRIN2A	p.Ala716Asp	S2	c.2147C>A	NM_000833.4	0	trans	RE+verbal dyspra
GRIN2A	p.Phe728Leu	S2	c.2184C>G	NM_000833.4	0		
GRIN2A	p.Asp731His	S2	c.2191G>C	NM_000833.4	0		
GRIN2A	p.Thr749Ile	S2	?	NM_000833.4	0	DM	
GRIN2A	p.Gly753Ala	S2	c.2258G>C	NM_000833.4	0		
GRIN2A	p.Gly760Ser	S2	c.2278G>A	NM_000833.3	0		
GRIN2A	p.Ile763Thr	S2	c.2288T>C	NM_000833.4	0		
GRIN2A	p.Leu779fsX5	S2	c.2334_2338delCTTGC	NM_000833.4	0	trans	ABPE; ADHD CSW
GRIN2A	p.Met817Thr	M4	c.2450T>C	NM_000833.3	0	DM	ID; EPI
GRIN2A	p.Met817Arg	M4	c.2450T>G	NM_000833.3	0		
GRIN2A	p.Ala818Thr	M4	c.2452G>A	NM_000833.3	0		
GRIN2A	p.Val820Gly	M4	c.2459T>G	NM_000833.4	0		
GRIN2A	p.Leu830ProX2	M4	c.2488dupC	NM_000833.4	0		
GRIN2A	p.His839Gln	CTD	c.2517C>A	NM_000833.4	0		

GRIN2A	p.Phe849Cys	CTD	c.2546T>G	NM_000833.4	0		
GRIN2A	p.Thr850Met	CTD	c.2549C>T	NM_000833.4	0		
GRIN2A	p.Val852Leu	CTD	c.2554G>T	NM_000833.4	0		
GRIN2A	p.Gly858Ala	CTD	c.2573G>C	NM_000833.3	0		
GRIN2A	p.Val935Phe	CTD	c.2803G>T	NM_000833.4	0		
GRIN2A	p.Gln950Ter	CTD	c.2848C>T	NM_000833.3	0		
GRIN2A	p.Gln964LysfsX38	CTD	c.2890delC	NM_000833.4	0	unk	EPI; LD
GRIN2A	p.Ala968Thr	CTD	c.2902G>A	NM_000833.3	0		SCZ
GRIN2A	p.Val1000Met	CTD	c.2998G>A	NM_000833.4	0	trans	ASD
GRIN2A	p.Tyr1051Asn	CTD	c.3151T>A	NM_000833.4	0		
GRIN2A	p.Thr1082Ile	CTD	c.3245C>T	NM_000833.3	0		
GRIN2A	p.Arg1088Thr	CTD	c.3263G>C	NM_000833.4	0		
GRIN2A	p.Asp1115Val	CTD	c.3344A>T	NM_000833.4	0		
GRIN2A	p.Phe1234fsX51	CTD	c.3701delT	NM_000833.4	0		
GRIN2A	p.Arg1241Gln	CTD	c.3722G>A	NM_000833.3	0		
GRIN2A	p.Asp1251Asn	CTD	c.3751G>A	NM_000833.4	0	DM; trans	RE; absense epile
GRIN2A	p.Asp1385Tyr	CTD	c.4153G>T	NM_000833.3	0		
GRIN2A	p.Tyr1387Ter	CTD	c.4161C>A	NM_000833.4	0	DM	CSWSS; begning
GRIN2A	p.Asn1397GlnX23	CTD	c.4189_4193delAATGA	NM_000833.3	0	DM	EPI; ID
GRIN2A	p.Met133Val	ATD	c.397A>G	NM_000833.4	1		
GRIN2A	p.Ser311Tyr	ATD	c.932C>A	NM_000833.4	1		
GRIN2A	p.Ile422Thr	S1	c.1265T>C	NM_000833.4	1		
GRIN2A	p.Arg431Ser	S1	c.1293G>C	NM_000833.4	1		

GRIN2A	p.Asn432Ser	S1	c.1295A>G	NM_000833.4	1		
GRIN2A	p.Lys438Asn	S1	c.1314G>C	NM_000833.4	1		
GRIN2A	p.Phe439Ile	S1	c.1315T>A	NM_000833.4	1		
GRIN2A	p.Asn444Ser	S1	c.1331A>G	NM_000833.4	1		
GRIN2A	p.Asn447Ile	S1	c.1340A>T	NM_000833.4	1		
GRIN2A	p.Phe459Leu	S1	c.1377C>G	NM_000833.4	1		
GRIN2A	p.Asp462Glu	S1	c.1386T>A	NM_000833.4	1		
GRIN2A	p.Ile463Ser	S1	c.1388T>G	NM_000833.4	1		
GRIN2A	p.Thr470Asn	S1	c.1409C>A	NM_000833.4	1		
GRIN2A	p.Val471Met	S1	c.1411G>A	NM_000833.4	1		
GRIN2A	p.Tyr478His	S1	c.1432T>C	NM_000833.4	1		
GRIN2A	p.Thr481Ile	S1	c.1442C>T	NM_000833.3	1		
GRIN2A	p.Asn491Asp	S1	c.1471A>G	NM_000833.4	1		
GRIN2A	p.Gly498Ala	S1	c.1493G>C	NM_000833.4	1		
GRIN2A	p.Glu520Val	S1	c.1559A>T	NM_000833.4	1		
GRIN2A	p.Val521Met	S1	c.1561G>A	NM_000833.4	1		
GRIN2A	p.Val559Met	M1	c.1675G>A	NM_000833.4	1		
GRIN2A	p.Met564Val	M1	c.1690A>G	NM_000833.4	1		
GRIN2A	p.val568Leu	M1	c.1702G>C	NM_000833.3	1		
GRIN2A	p.Phe576Leu	M1	c.1728T>A	NM_000833.4	1		
GRIN2A	p.Gly583Arg	M1-M2	c.1747G>A	NM_000833.4	1		
GRIN2A	p.Ala589Gly	M1-M2	c.1766C>G	NM_000833.4	1		
GRIN2A	p.Gly591Arg	M1-M2	c.1771G>A	NM_000833.4	1		

GRIN2A	p.Pro594Leu	M1-M2	c.1781C>T	NM_000833.4	1		
GRIN2A	p.Gly596Arg	M1-M2	c.1786G>A	NM_000833.4	1		
GRIN2A	p.Ile601Thr	M2	c.1802T>C	NM_000833.4	1		
GRIN2A	p.Leu607Val	M2	c.1819C>G	NM_000833.4	1		
GRIN2A	p.Met630Val	M3	c.1888A>G	NM_000833.4	1		
GRIN2A	p.Gln671His	S2	c.2013G>C	NM_000833.3	1		
GRIN2A	p.Pro673Thr	S2	c.2017C>A	NM_000833.4	1		
GRIN2A	p.His674Gln	S2	c.2022T>G	NM_000833.4	1		
GRIN2A	p.Thr706Ile	S2	c.2117C>T	NM_000833.4	1		
GRIN2A	p.Ser719Arg	S2	c.2157C>G	NM_000833.4	1		
GRIN2A	p.Asp742Glu	S2	c.2226T>G	NM_000833.4	1		
GRIN2A	p.Ile755Val	S2	c.2263A>G	NM_000833.4	1		
GRIN2A	p.Phe756Tyr	S2	c.2267T>A	NM_000833.4	1		
GRIN2A	p.Arg773Lys	S2	c.2318G>A	NM_000833.4	1		
GRIN2A	p.Val783Ala	S2	c.2348T>C	NM_000833.4	1		
GRIN2A	p.Met788Ile	S2	c.2364G>A	NM_000833.4	1		
GRIN2A	p.Ile836Leu	M4	c.2506A>C	NM_000833.4	1		
GRIN2A	p.Gly851Arg	CTD	c.2551G>C	NM_000833.4	1		
GRIN2A	p.Cys853Arg	CTD	c.2557T>C	NM_000833.4	1		
GRIN2A	p.Arg865Thr	CTD	c.2594G>C	NM_000833.4	1		
GRIN2A	p.Ser869Arg	CTD	c.2607C>A	NM_000833.4	1		
GRIN2A	p.Met894Ile	CTD	c.2682G>A	NM_000833.4	1		
GRIN2A	p.Thr965Ile	CTD	c.2894C>T	NM_000833.4	1		

GRIN2A	p.Asp1249Asn	CTD	c.3745G>A	NM_000833.3	1		
GRIN2A	p.Trp1271Ter	CTD	c.3813G>A	NM_000833.4	1	unk	not provided
GRIN2A	p.Ser1341Arg	CTD	c.4023C>G	NM_000833.4	1		
GRIN2A	p.Ala290Val	ATD	c. 869C>T				RE
GRIN2A	p.Gly295Ser	ATD					RE
GRIN2A	p.Arg370Trp	ATD					RE
GRIN2A	p.Arg681*	S2				trans	LKS (proband); ID
GRIN2A		-	c.2008-32_c.2008-31dupCT	Het			
GRIN2A		-	Exon 4 & 5				
GRIN2A		-	t (16;17) (p13;q11)			trans	FS + GTCS + Seve difficulties (fathe
GRIN2A		-	c.414+7C>T			trans	IS
GRIN2A	p.Ile876Thr	CTD	c.2627T>C				temp lobe epilep
GRIN2A	p.Val967Leu	CTD	c.2899G>C				temp lobe epilep temp spikes
GRIN2A	p.Thr1064Ala	CTD	c.3190A>G				SCZ; EPI; begning
GRIN2A	p.Asn1076Lys	CTD	c.3228C>G				benign epi w cen
GRIN2A	p.Ile1379Val	CTD	c.4135A>G				Juvenile Absence

Phenotypes: ADHD, attention deficit hyperactivity disorder; AGL , Angelman-like phenotype; ASD, autism spectrum disorder; BP, bipolar disorder; DD, developmental delay; EPI, epilepsy, seizures; HPT, hypotonia; ID, intellectual disability (includes non-verbal); IS, infantile spasms; LD, language disorders (delay, dyspaxia, apraxia, aphasia); LGS, Lennox-Gastaut Syndrome; LKS, Landau-Kleffner syndrome; MC, microcephaly; MD, movement disorder; Rett, Rett-like syndrome; SCZ, schizophrenia; WS, West Syndrome. **Domains**: ATD, amino terminal domain; CTD, carboxyl terminal domain; S1, S2, agonist binding domain; M1-M4, membrane domains; DM,							

de novo; trans, transmitted.							

Functional Data represent fold changes in receptor activity by gene variant. For example, -2.3 is a 2.3 fold decrease in variant receptor activity compared to wild-type (no mutation) control. A "0" means no change from wild-type; ‡ indicates variant receptor current too small, unable to measure endpoint activity; Glu, Glutamate; Gly, Glycine; Mg2+, magnesium; Zn2+, zinc								

841

842